DOI: 10.1534/genetics.110.125567

A Genome-Wide Enhancer Screen Implicates Sphingolipid Composition in Vacuolar ATPase Function in *Saccharomyces cerevisiae*

Gregory C. Finnigan,* Margret Ryan* and Tom H. Stevens*,[1]

*Institute of Molecular Biology, University of Oregon, Eugene, Oregon 97403

Manuscript received December 1, 2010
Accepted for publication December 23, 2010

ABSTRACT

The function of the vacuolar H^+-ATPase (V-ATPase) enzyme complex is to acidify organelles; this process is critical for a variety of cellular processes and has implications in human disease. There are five accessory proteins that assist in assembly of the membrane portion of the complex, the V_0 domain. To identify additional elements that affect V-ATPase assembly, trafficking, or enzyme activity, we performed a genome-wide enhancer screen in the budding yeast *Saccharomyces cerevisiae* with two mutant assembly factor alleles, *VMA21* with a dysfunctional ER retrieval motif (*vma21QQ*) and *vma21QQ* in combination with *voa1*Δ, a nonessential assembly factor. These alleles serve as sensitized genetic backgrounds that have reduced V-ATPase enzyme activity. Genes were identified from a variety of cellular pathways including a large number of trafficking-related components; we characterized two redundant gene pairs, *HPH1/HPH2* and *ORM1/ORM2*. Both sets demonstrated synthetic growth defects in combination with the *vma21QQ* allele. A loss of either the *HPH* or *ORM* gene pairs alone did not result in a decrease in vacuolar acidification or defects in V-ATPase assembly. While the Hph proteins are not required for V-ATPase function, Orm1p and Orm2p are required for full V-ATPase enzyme function. Consistent with the documented role of the Orm proteins in sphingolipid regulation, we have found that inhibition of sphingolipid synthesis alleviates Orm-related growth defects.

THE vacuolar H^+-ATPase (V-ATPase) is a multisubunit complex that is highly conserved across eukaryotes (Graham *et al.* 2003). It functions to actively acidify cellular compartments by coupling the hydrolysis of ATP to the translocation of protons across membranes through a conserved rotary mechanism (Hirata *et al.* 2003; Yokoyama *et al.* 2003; Imamura *et al.* 2005). Organelle acidification plays a crucial role in various cellular functions such as vesicular trafficking, endocytosis, neurotransmitter uptake, membrane fusion, and ion homeostasis (Kane 2006; Forgac 2007). Specialized isoforms of the V-ATPase complex can be found on different cellular membranes including the plasma membrane (Forgac 2007). A number of human diseases have been associated with or directly linked to defects in the V-ATPase complex: osteopetrosis (Frattini *et al.* 2000), renal tubular acidosis (Karet *et al.* 1999), and cancer cell migration (Martinez-Zaguilán *et al.* 1999). The V-ATPase is an essential complex for all eukaryotes with the exception of some fungi.

The budding yeast *Saccharomyces cerevisiae* requires the V-ATPase to survive under specific environmental conditions, including alkaline conditions or otherwise toxic levels of metals (Eide *et al.* 2005; Kane 2006). Yeast utilize the proton gradient created by the V-ATPase to drive sequestration of Ca^{2+} and Zn^{2+} ions within the vacuole (Klionsky *et al.* 1990). A variety of proton-exchange antiporter pumps reside on the vacuolar membrane and other organelles that participate in maintaining nontoxic cytosolic levels of various ions and metals including calcium and zinc (Miseta *et al.* 1999; MacDiarmid *et al.* 2002). Deletion of any of the V-ATPase component proteins results in a number of specific growth and cellular phenotypes, including sensitivity to excess metals and a lack of vacuolar acidification. This makes yeast a useful model system to study the V-ATPase complex (Graham *et al.* 2003; Kane 2006). Complete disruption of V-ATPase function in yeast results in a characteristic Vma^- phenotype: failure to grow on media buffered to pH 7.5 (Kane 2006). Additionally, numerous genetic screens have demonstrated that a loss of the V-ATPase renders yeast sensitive to a variety of metals (including zinc and calcium) and drugs (Eide *et al.* 2005; Kane 2007). Yeast lacking the V-ATPase complex do not acidify their vacuoles as shown through a lack of quinacrine staining (Weisman *et al.* 1987).

The V-ATPase enzyme in yeast contains 14 protein subunits within two domains: the V_1 portion is responsible for hydrolyzing ATP, and the V_0 portion

Supporting information is available online at http://www.genetics.org/cgi/content/full/genetics.110.125567/DC1.

[1]*Corresponding author:* Institute of Molecular Biology, University of Oregon, Eugene, OR 97403-1229. E-mail: stevens@molbio.uoregon.edu

shuttles protons across a lipid bilayer (Forgac 2007). The V_1 domain (subunits A–H) is peripherally associated, and the V_0 domain (subunits a, d, e, c, c′, and c′′) is imbedded within the membrane except subunit d, which is a peripheral membrane protein. The functional V-ATPase enzyme requires the presence of all of these subunits. Subunit a has two isoforms in yeast, the absence of one of them is not sufficient to cause a Vma⁻ phenotype. Yeast contain two populations of the V-ATPase complex and their localization is dictated by the incorporation of one of two isoforms of subunit a, Stv1p or Vph1p (Manolson *et al.* 1992, 1994). While higher eukaryotes contain numerous isoforms for many of the different V-ATPase subunits (Marshansky and Futai 2008), Stv1p/Vph1p is the only structural difference between the two yeast enzymes. V-ATPase complexes containing the Vph1 protein are trafficked to the vacuolar membrane while Stv1p-containing V-ATPases are retained within the Golgi/endosomal network (Manolson *et al.* 1994). Similarly, higher eukaryotes use different isoforms of subunit a to direct the localization of the V-ATPase to specific cellular compartments (Forgac 2007). One mechanism of V-ATPase regulation occurs through the rapid, reversible dissociation of the V_1 and V_0 domains (Kane 2006).

In the absence of any V_1 subunit, the V_0 domain is still properly assembled and targeted to the vacuole (Graham *et al.* 2003). In the absence of the V_0 domain, V_1 is still assembled (Tomashek *et al.* 1997). Loss of any V_0 subunit protein prevents proper V_0 assembly and ER exit (Graham *et al.* 2003), and Vph1p undergoes ubiquitin-dependent ER-associated degradation (ERAD) (Hill and Cooper 2000). Assembly of the V_0 domain occurs in the ER and requires the presence of a number of additional proteins (Forgac 2007). Five ER-localized assembly factors have been identified in yeast that are required for full V-ATPase function yet are not part of the final complex: Vma21p, Vma22p, Vma12p, Pkr1p, and Voa1p (Hirata *et al.* 1993; Hill and Stevens 1995; Malkus *et al.* 2004; Davis-Kaplan *et al.* 2006; Ryan *et al.* 2008). Deletion of *VMA21*, *VMA12*, or *VMA22* causes a failure of the V_0 subunits to properly assembly in the ER and a complete loss of V-ATPase function, resulting in a full Vma⁻ phenotype (Graham *et al.* 2003). Yeast lacking *PKR1* show a limited amount of V_0 assembly (Davis-Kaplan *et al.* 2006) and yeast lacking *VOA1* display only a slight reduction in V-ATPase enzyme activity (Ryan *et al.* 2008). Consequently, *pkr1*Δ cells score a partial Vma⁻ phenotype while *voa1*Δ cells appear normal.

Genetic screens in *S. cerevisiae* have been critical in identifying the components of the V-ATPase and its associated factors (Ohya *et al.* 1991; Ho *et al.* 1993; Sambade *et al.* 2005). However, the most recently discovered V-ATPase assembly factor, Voa1p, was identified by proteomics and *voa1*Δ cells have no detectable growth phenotype (Ryan *et al.* 2008). Voa1p physically associates with the Vma21p-V_0 complex early in V-ATPase assembly and deletion of *VOA1* displays a dramatic growth phenotype in conjunction with a specific mutant allele of the *VMA21* assembly factor, *vma21QQ* (Ryan *et al.* 2008). In yeast, it has been shown that Vma21p plays a critical role in V-ATPase assembly and chaperones the completed V_0 subcomplex out of the ER to the Golgi (Hill and Stevens 1994; Malkus *et al.* 2004). Vma21p is retrieved back to the ER through a conserved, C-terminal dilysine motif and participates in multiple rounds of assembly and transport (Hill and Stevens 1994; Malkus *et al.* 2004). Mutation of the dilysines to diglutamine residues, as in *vma21QQ*, results in mislocalization of yeast Vma21p to the vacuolar membrane and a significant loss of V-ATPase function.

The identification of V-ATPase assembly factors like Voa1p that do not display a full Vma⁻ are not likely to be found using traditional forward genetic screens. Also, pathways involved in promoting full V-ATPase function may act independently of V_1 and/or V_0 assembly and require a sensitized genetic background to produce a detectible growth phenotype. However, *vma21QQ* mutant yeast and, more so, the *vma21QQ voa1*Δ double mutant are two cases where the V-ATPase is partially compromised for function (Hill and Stevens 1994; Ryan *et al.* 2008). We have chosen to use these two assembly mutants in genome-wide enhancer screens to identify additional factors that assist in promoting full V-ATPase function by searching for genes that will cause an increase in calcium or zinc sensitivity when deleted.

Here we report the identification of *HPH1* and *ORM2* in a genome-wide search for V-ATPase effectors. We describe the characterization of these two redundant yeast gene pairs, *HPH1/HPH2* and *ORM1/ORM2*, both of which display synthetic growth defects when deleted in combination with the *vma21QQ* mutant. Both sets of genes were found to have specific growth phenotypes on zinc and calcium media. Deletion of either gene pair did not affect vacuolar acidification or assembly of the V_0 domain. However, deletion of *ORM1* and *ORM2* results in a reduction of V-ATPase activity. The Orm proteins have very recently been shown to be negative regulators of sphingolipid synthesis (Breslow *et al.* 2010; Han *et al.* 2010). Consistent with these reports, we find that disruption of sphingolipid biogenesis is able to suppress Orm-related growth defects.

MATERIALS AND METHODS

Plasmids and yeast strains: Bacterial and yeast manipulations were done using standard laboratory protocols for molecular biology (Sambrook and Russel 2001). Plasmids for this study are listed in Table 1. *ORM1* plus flanking sequence was amplified by polymerase chain reaction (PCR) from BY4741 (Invitrogen, Carlsbad, CA) genomic DNA using primers containing an upstream *Bam*HI restriction site and downstream *Sal*I restriction site. This fragment was inserted into pCR4Blunt-TOPO (Invitrogen), digested, and ligated

TABLE 1

Plasmids used in this study

Plasmid	Description	Reference
pRS415	*CEN, LEU2*	Simons *et al.* (1987)
pRS316	*CEN, URA3*	Sikorski and Hieter (1989)
YEp351	*2μ, LEU2*	Hill *et al.* (1986)
pGF127	YEp351 *ORM1*	This study
pGF87	pRS415 *VPH1::GFP::Sp_HIS5*	This study
pGF06	pRS316 *VPH1::GFP::Sp_HIS5*	Ryan *et al.* (2008)
pGF20	pRS316 *VMA2::mCherry::Nat^R*	This study

into the *Bam*HI and *Sal*I sites of YEp351 to create pGF127. pGF87 was created using homologous recombination and *in vivo* ligation by gapping pRS415 and cotransforming a PCR fragment containing *prVPH1::VPH1::GFP::Sp_HIS5* (amplified from pGF06) with flanking sequence to the pRS415 vector.

Yeast strains used in this study are listed in Table 2. GFY164 was created by PCR amplifying the *hph1Δ::Kan^R* cassette plus 500 bp flanking sequence from corresponding BY4741 strains of the genome deletion collection (Open Biosystems, Huntsville, AL). It was subcloned into pCR4Blunt-TOPO, reamplified by PCR, transformed into SF838-1Dα, and selected on YEPD plus G418 (Gold Biotechnology, St. Louis, MO). Strains containing deletion cassettes other than Kan^R (Hyg^R or Nat^R) were created by PCR amplifying either the Hyg^R or Nat^R cassette from pAG32 or pAG25, respectively (Goldstein and McCuster 1999) and transforming the fragment into the corresponding Kan^R genome deletion strain to exchange drug resistance markers. Deletions in the SF838-1Dα strain (GFY164, GFY165, GFY166, GFY168, GFY169, and GFY170) were constructed by PCR amplifying the appropriate gene locus (including 500 bp of 5′-UTR and 3′-UTR flanking sequence), transforming into wild-type (WT) SF838-1Dα, and selecting for the appropriate drug resistance. GFY167, GFY171, and GFY172 were created using LGY183 as the parental strain. GFY173 was created using MRY5 as the parental strain. All deletion strains in SF838-1Dα were confirmed by diagnostic PCR from genomic DNA with primers complementary to the 5′-UTR (750–1000 bp upstream of the start codon) and internal to the drug resistance gene. A disruption cassette was created to delete *TSC3* by first PCR amplifying the *TSC3* open reading frame with 500 bp of flanking UTR, subcloning in pCR4Blunt-TOPO, and introducing a unique restriction site within the ORF. The *TSC3* gene was subcloned into pRS316 and the entire ORF was replaced by the Nat^R cassette using homologous recombination. The deletion cassette was amplified and cloned into pCR4Blunt-TOPO for use in creating both GFY174 (using SF838-1Dα as the parental strain), GFY175 (using GFY170 as the parental strain), and GFY313 (using MRY5 as the parental strain). pGF20 was created by first swapping GFP for mCherry (Shaner *et al.* 2004) in pRS316 *VMA2-GFP* and introducing a unique *Pme*I restriction site downstream of mCherry using site-directed mutagenesis. Second, *in vivo* ligation was used to insert the *ADH1* terminator and Nat^R cassette at the 3′ end of *VMA2*-mCherry. A single, C-terminal mCherry (PCR amplified from pGF20 including the Nat^R cassette) was integrated at the *VMA2* locus in strains GFY170, SF838-1Dα, and TASY006. This created yeast strains GFY302, GFY304, and GFY305, respectively.

The synthetic genetic array (SGA) query strains were created from yeast parental strain Y7092 (Tong and Boone 2006). After PCR amplifying the *vma21QQ::HA::Nat^R* locus with 500 bp of flanking sequence from GFY163 genomic DNA, the PCR product was transformed into Y7092 to create GFY36. To create GCY3, GCY2 (*vma21QQ::HA voa1Δ::Kan^R*) was transformed with the Nat^R cassette to replace the Kan^R cassette. Both the *VMA21* and *VOA1* loci were PCR amplified with flanking sequence and the PCR product was transformed into Y7092. GFY104 was created by PCR amplifying both the *VMA21* and *VOA1* loci from MRY5 (*vma21QQ::HA voa1::Hyg^R*) with 500 bp of flanking sequence and transforming the fragment into GCY3.

Culture conditions: Yeast were cultured in YEPD (1% yeast extract, 2% peptone, and 2% dextrose), YEPD buffered to pH 5.0 using 50 mm succinate/phosphate plus 0.01% adenine, or synthetic minimal media with dextrose (SD) and the appropriate amino acids. Growth tests were performed by culturing exponentially growing yeast in rich medium to a cell density of 1.0 OD_{600}, serially diluted fivefold, and spotted onto agar plates. Plates used included YEPD pH 5.0, YEPD + 4.0 mm or 5.0 mm $ZnCl_2$, YEPD + 100 mm $CaCl_2$, and YEPD + 25 mm or 50 mm $CaCl_2$ pH 7.5 (using 50 mm HEPES).

Synthetic genetic array screen: A synthetic genetic enhancer screen was performed as previously described (Tong *et al.* 2001; Tong and Boone 2006). Briefly, the query strains (GFY36, GCY3, and GFY104) were mated to the *MAT***a** haploid genome deletion collection (BY4741, *his3Δ1 leu2Δ0, met15Δ0, ura3Δ0*) and double or triple haploid mutants were selected. The final haploid mutant array was spotted onto YEPD pH 5.0, YEPD + $ZnCl_2$, or YEPD + $CaCl_2$ pH 7.5 and incubated at 30° for 2–3 days. Scans of each plate were visually scored for colony size on each plate type used; colonies were scored for increased sensitivity to calcium or zinc. The genome deletion collection was also arrayed under identical conditions and scored in the same way. Colonies that showed equivalent sensitivity to either metal as a single deletion strain and as part of the double (or triple) mutant collection were not scored as positive hits. Only mutants that displayed a synthetic growth defect that was not present (or not as strong) in either of the single mutant strains were scored as positive hits. Gene ontology (GO) analysis was performed using the Saccharomyces Genome Database (SGD) GO term finder (version 0.83) using a *P*-value cutoff of 0.01.

Whole cell extract preparation and immunoblotting: Whole cell extracts were prepared as previously described (Ryan *et al.* 2008). Briefly, cultures were grown overnight in SD dropout media and then diluted to 0.25 OD_{600}/ml in YEPD pH 5.0 and grown to a cell density of $OD_{600} = 1.0$. A total of 10 OD_{600} of the culture was centrifuged, resuspended in 0.25 ml Thorner buffer (8 m urea, 5% SDS, and 50 mm TRIS pH 6.8), and vortexed with 0.2 ml of glass beads. Following centrifugation, protein concentrations were determined using a modified Lowry protein assay (Markwell *et al.* 1978). Equal amounts of protein were separated by SDS–PAGE, transferred to nitrocellulose membrane, and probed with antibodies. Antibodies used

TABLE 2

Strains used in this study

Strain	Genotype	Reference
SF838-1Dα	*MATα ura3-52 leu2-3,112 his4-519 ade6 pep4-3 gal2*	Rothman and Stevens (1986)
Y7092	*MATα can1Δ::prSTE2-Sp_HIS5 lyp1Δ ura3Δ0 leu2Δ0 his3Δ1 met15Δ0 LYS2*	Tong and Boone (2006)
GFY36	Y7092; *vma21QQ::HA::Nat^R*	This study
GCY2	Y7092; *vma21QQ::HA voa1Δ::Kan^R*	This study
GCY3	Y7092; *vma21QQ::HA voa1Δ::Nat^R*	This study
GFY104	Y7092; *vma21QQ::HA voa1::Hyg^R*	This study
TASY006	SF838-1Dα; *vma21Δ::Kan^R*	Compton *et al.* (2006)
LGY183	SF838-1Dα; *vma21QQ::HA*	Ryan *et al.* (2008)
MRY5	SF838-1Dα; *vma21QQ::HA voa1::Hyg^R*	Ryan *et al.* (2008)
MRY14	SF838-1Dα; *voa1::Hyg^R*	Ryan *et al.* (2008)
GFY163	SF838-1Dα; *vma21QQ::HA::Nat^R*	This study
GFY164	SF838-1Dα; *hph1Δ::Kan^R*	This study
GFY165	SF838-1Dα; *hph2Δ::Kan^R*	This study
BY4741	*MAT***a** *leu2Δura3Δ met15Δ his3Δ*	Yeast Deletion Collection
GFY181	BY4741; *hph1Δ::Kan^R hph2Δ::Hyg^R*	This study
GFY166	SF838-1Dα; *hph1Δ::Kan^R hph2Δ::Hyg^R*	This study
GFY167	SF838-1Dα; *vma21QQ::HA hph1Δ::Kan^R hph2Δ::Nat^R*	This study
GFY168	SF838-1Dα; *orm1Δ::Kan^R*	This study
GFY169	SF838-1Dα; *orm2Δ::Kan^R*	This study
GFY170	SF838-1Dα; *orm1Δ::Hyg^R orm2Δ::Kan^R*	This study
GFY171	SF838-1Dα; *vma21QQ::HA orm2Δ::Kan^R*	This study
GFY172	SF838-1Dα; *vma21QQ::HA orm1Δ::Hyg^R orm2Δ::Kan^R*	This study
GFY173	SF838-1Dα; *vma21QQ::HA voa1::Hyg^R hph1Δ::Kan^R*	This study
GFY174	SF838-1Dα; *tsc3Δ::Nat^R*	This study
GFY175	SF838-1Dα; *orm1ΔHyg^R orm2Δ::Kan^R tsc3Δ::Nat^R*	This study
GFY304	SF838-1Dα; *VMA2::mCherry::Nat^R*	This study
GFY305	SF838-1Dα; *VMA2::mCherry::Nat^R vma21Δ::Kan^R*	This study
GFY302	SF838-1Dα; *VMA2::mCherry::Nat^R orm1Δ::Hyg^R orm2Δ::Kan^R*	This study
GFY313	SF838-1Dα; *vma21QQ::HA voa1::Hyg^R tsc3Δ::Nat^R*	This study

included monoclonal primary anti-Vph1p (10D7; Invitrogen), anti-Vma1p (8B1; Invitrogen), and anti-Dpm1p (5C5; Invitrogen), and secondary horseradish peroxidase-conjugated anti-mouse antibody (Jackson ImmunoResearch Laboratories, West Grove, PA). Blots were visualized by ECL detection.

Fluorescence microscopy: Yeast were stained with quinacrine as previously described (Flannery *et al.* 2004). Briefly, cells were grown overnight in YEPD pH 5.0 plus adenine, and diluted to a cell density of 0.25 OD_{600}/ml in YEPD. Yeast were harvested at a density of 0.8–1.0 OD_{600}/ml and 1 ml of culture was placed on ice for 5 min. Cells were pelleted and resuspended in 200 μm quinacrine, 100 mm Hepes pH 7.6, and 50 μg/ml of concanavalin A tetramethylrhodamine (Invitrogen) in YEPD for 10 min at 30°. Following staining with quinacrine, cells were placed on ice and washed three times in 100 mm Hepes pH 7.6 plus 2% glucose (4°). Microscopy images were obtained using an Axioplan 2 fluorescence microscope (Carl Zeiss, Thornwood, NY). A ×100 objective was used as well as AxioVision software (Carl Zeiss).

V-ATPase activity assay: Yeast vacuoles were isolated from wild-type (SF838-1Dα and BY4741), *vma21Δ::Kan^R* (TASY006), *vma21QQ::HA* (LGY183), *orm1Δ::Hyg^R orm2Δ::Kan^R* (GFY170), *vma21QQ::HA voa1::Hyg^R* (MRY5), *vma21QQ::HA orm1Δ::Hyg^R orm2Δ::Kan^R* (GFY172), and *hph1Δ::Kan^R hph2Δ::Hyg^R* (GFY166 and GFY181) strains as previously published (Uchida *et al.* 1985). Modifications to this protocol included harvesting cells at 1.8–2.2 OD_{600}/ml and use of a tighter-fitting dounce homogenizer (five strokes). Fresh vacuoles were assayed by a coupled spectrophotometric assay (Conibear and Stevens 2002). In this assay system, ATP hydrolysis is coupled to NADH oxidation (340 nm) in a reaction mixture containing 50 μg/ml vacuole membrane protein, 25 mm MES, 25 mm MOPS, 25 mm KCl, 5 mm $MgCl_2$, 1 mm NaN_3, 0.05 mm Na_3VO_4, 2 mm phosphoenolpyruvate, 0.5 mm NADH, 30 units/ml pyruvate kinase, and 37 units/ml lactate dehydrogenase; pH 7 (KOH), with and without 1 μm concanamycin A. Reactions were initiated by adding Mg^{2+}-ATP to 2 mm and thermostatted at 30°. For each mutant strain, one to three separate vacuole preparations were assayed, and the assay was repeated two to six times for each preparation. Concanamycin A-sensitive ATPase activities were determined by calculating the activity as a percentage of wild-type activity for each biological replicate. For samples with multiple vacuole preparations, these percentages were averaged and the error was presented as the standard error of the mean. For samples with only a single biological preparation, the error is presented as the standard deviations for replicate assays.

RESULTS

Genome-wide SGA screen for V-ATPase effectors: To identify new genes that assist in promoting full V-ATPase function, we performed three SGA Vma$^-$ enhancer screens using the *S. cerevisiae* haploid deletion mutant collection (4741 mutants). Since a loss of *VOA1* only displayed a synthetic growth defect upon combination with the *vma21QQ* mutation, additional

factors might only be identified in a sensitized genetic background. The three query mutants used were *vma21QQ::Nat*^{R}, *vma21QQ voa1*Δ*::Nat*^{R}, and *vma21QQ voa1::Hyg*^{R} (subsequent experiments were all performed with the *voa1::Hyg*^{R} allele, designated as *voa1*Δ). The *VMA21* and *VOA1* loci are tightly linked; only 146 bp separate their open reading frames. We chose to use both mutants containing the *VOA1* disruption as it has been shown that a complete deletion of this open reading frame results in a decrease in the steady-state levels of Vma21p, whereas the *voa1::Hyg*^{R} allele does not lower Vma21p levels (Ryan *et al.* 2008). Therefore, the *voa1*Δ*::Nat*^{R} allele served as an additional sensitized genetic background.

Yeast that contain Vma21p having the mutated retrieval/retention signal, *vma21QQ*, show a partial growth defect on elevated calcium media buffered to pH 7.5 and have reduced V-ATPase activity (Hill and Stevens 1994; Ryan *et al.* 2008). Additionally, *vma21QQ voa1*Δ yeast are also compromised for V-ATPase function yet do not display a full Vma$^-$ phenotype (Ryan *et al.* 2008).

The haploid double or triple mutant yeast were plated onto rich media and media containing either zinc (2.75 mM or 7.0 mM) or calcium (50 mM or 100 mM) buffered to pH 7.5 in quadruplicate. Yeast that displayed increased sensitivity to these conditions were scored as positive hits. Genes were identified from a diverse set of cellular processes such as protein modification, metabolism, chromatin remodeling, and transcriptional regulation (Figure 1 and supporting information, Table S1). A comprehensive GO analysis was performed for categories of genes that were enriched in our SGA screens (Table S2). Some of the most highly enriched categories included vacuolar transport (P-value of 4.94×10^{-17}), vesicle-mediated transport (P-value of 3.48×10^{-15}), and intracellular transport (P-value of 9.46×10^{-10}). Genes identified by the three SGA screens that correspond to elements of protein trafficking, vacuolar morphology, and the V-ATPase complex are listed in Table 3 and several were chosen for further study.

Since we were searching for genes that showed increased sensitivity to zinc or calcium when deleted in combination with *vma21QQ* or *vma21QQ voa1*Δ, we did not identify any of the essential V-ATPase subunits or assembly factors (those with a *VMA* designation) as expected. Also, *VOA1* was not identified in the *vma21QQ* SGA screen because it is genetically linked to the *VMA21* locus. For the *voa1*Δ locus to be paired with the *vma21QQ* mutation during the SGA protocol, a crossover event would be required between these two loci. However, we did identify V-ATPase subunits *VPH1*, *STV1*, the assembly factor *PKR1*, and genes within the vacuolar transporter chaperone (VTC) and regulator of vacuolar and endosomal membrane (RAVE) complexes.

In addition, genes involved in ER-resident processes including protein folding and degradation were identified (Table 3). A number of genes were found that have been poorly characterized according to the SGD and these were most interesting to us. We chose to examine Orm2p for further study because it was an ER-localized, integral membrane protein. Also, Hph1p has been identified as an ER-localized binding partner of calcineurin (Heath *et al.* 2004). Due to the genetic link between calcineurin and the V-ATPase (Tanida *et al.* 1995), we also chose *HPH1* for further study.

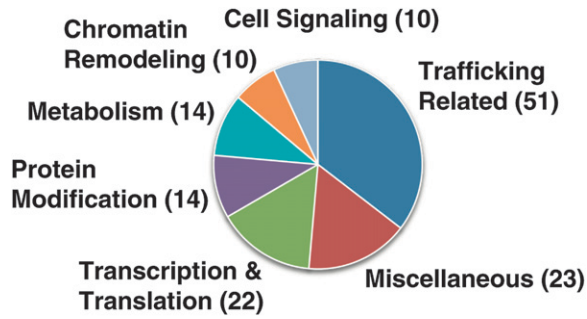

Figure 1.—Molecular function of 144 genes identified in at least two of three SGA screens for an enhanced Vma$^-$ phenotype. Genes were categorized according to their presumed molecular function. The miscellaneous category includes lipids/sphingolipids, cellular morphogenesis, nuclear import, and several other processes, and also genes with no molecular characterization. A comprehensive list of all genes identified can be found in Table S1 and a comprehensive GO analysis can be found in Table S2.

***HPH1/HPH2* or *ORM1/ORM2* null mutants cause synthetic growth defects in *vma21QQ* yeast:** The *hph1*Δ mutation was moved to the SF838-1Dα genetic background and carefully tested by serial dilution in comparison to Vma$^-$ and Vma-compromised strains. The growth phenotypes of *vma21QQ voa1*Δ yeast deleted for *HPH1* were tested on media containing 50 mM calcium buffered to pH 7.5 (Figure 2A). Whereas wild-type yeast were able to grow under these conditions, yeast deleted for *VMA21* were unable to grow as they lack functional V-ATPase complexes. *vma21QQ voa1*Δ yeast showed a compromised level of growth under these conditions and a deletion of *HPH1* in this strain caused a further increase in sensitivity (Figure 2A). *HPH1* has a homolog in *S. cerevisiae*, *HPH2*, and both Hph1p and Hph2p reside in the ER membrane (Heath *et al.* 2004). It has been reported that deletions in *HPH1* and *HPH2* display a synthetic growth defect under alkaline conditions of pH 8.8 (Heath *et al.* 2004). Since a reduction in V-ATPase function results in increased sensitivity to calcium or zinc, we determined whether a loss of the *HPH* genes results in a metal-specific phenotype. Loss of either *HPH1* or *HPH2* did not result in any sensitivity to excess zinc yet deletion of both *HPH* genes caused a dramatic growth defect on 5.0 mM $ZnCl_2$ (Figure 2B). Both *HPH1* and *HPH2* were also deleted in a strain containing the *vma21QQ* mutation and tested on the less stringent conditions of 4.0 mM $ZnCl_2$. Both *vma21QQ* and *hph1*Δ *hph2*Δ yeast grew comparable to

TABLE 3

Genes identified by genome-wide SGA screens for V-ATPase effectors that are trafficking related or whose protein products are ER localized

Trafficking-related genes	
AP-3 (4)	*apl5*Δ, *apl6*Δ, *apm3*Δ, *aps3*Δ
Vesicle formation (5)	*arf1*Δ, *cdc50*Δ, *drs2*Δ, *vps1*Δ, *yap1801*Δ
Rabs/vesicle targeting factors (5)	*gyp1*Δ, *sro7*Δ, *vps21*Δ, *vps9*Δ, *ypt7*Δ
TGN trafficking (11)	*age2*Δ, *arl1*Δ, *arl3*Δ, *cog5*Δ, *cog6*Δ, *cog7*Δ, *cog8*Δ, *coy1*Δ, *gyp36*Δ, *sys1*Δ, *vps13*Δ
ESCRT/MVB sorting (13)	*vps2*Δ, *vps22*Δ, *vps23*Δ, *vps24*Δ, *vps25*Δ, *vps27*Δ, *vps36*Δ, *vps37*Δ, *vps4*Δ, *vps46*Δ, *vps55*Δ, *vps60*Δ, *vta1*Δ
Vacuole inheritance (2)	*cla4*Δ, *vac8*Δ
HOPS/CORVET (4)	*vam6*Δ, *vps3*Δ, *vps33*Δ, *vps41*Δ
Endocytosis/exocytosis (6)	*chs5*Δ, *chs6*Δ, *gsf2*Δ, *lst4*Δ, *rcy1*Δ, *drs2*Δ
ER-Golgi trafficking (12)	*bst1*Δ, *erd1*Δ, *erp3*Δ, *erv46*Δ, *gcs1*Δ, *get1*Δ, *get2*Δ, *get3*Δ, *gsg1*Δ, *pho86*Δ, *sec28*Δ, *ubp3*Δ
Autophagy (5)	*atg15*Δ, *atg21*Δ, *atg27*Δ, *atg8*Δ, *vps62*Δ
GARP (2)	*vps52*Δ, *vps53*Δ
SNAREs and fusion (8)	*gos1*Δ, *pep12*Δ, *sec22*Δ, *snx4*Δ, *swf1*Δ, *tlg2*Δ, *vam10*Δ, *vam7*Δ
Phosphatidylinositol synthesis (3)	*inp53*Δ, *sac1*Δ, *vac14*Δ
Retromer (5)	*vps17*Δ, *vps26*Δ, *vps29*Δ, *vps35*Δ, *vps5*Δ
H^+-V-ATPase (7)	*pkr1*Δ, *rav1*Δ, *rav2*Δ, *stv1*Δ, *vph1*Δ, *vtc1*Δ, *vtc4*Δ
Miscellaneous (5)	*apm1*Δ, *ccz1*Δ, *mon1*Δ, *vps19*Δ, *yck3*Δ
Genes whose protein products are ER localized	
Protein degradation (2)	*cue1*Δ, *ubc7*Δ
Protein import and maturation (5)	*cne1*Δ, *cwh41*Δ, *emc1*Δ, *scj1*Δ, *sec66*Δ
Miscellaneous (18)	*alg6*Δ, *alg8*Δ, *bsd2*Δ, *csg2*Δ, *erg3*Δ, *erg6*Δ, *flc2*Δ, ***hph1***Δ, *ice2*Δ, *ilm1*Δ, *mga2*Δ, ***orm2***Δ, *ost3*Δ, *ost4*Δ, *per1*Δ, *scs2*Δ, *spf1*Δ, *sur4*Δ

Genes found in our screens that are involved in either protein trafficking or are ER localized are listed above. A comprehensive list of all genes identified in all three screens can be found in Table S1. Screens were performed with query strains *vma21QQ voa1::Hyg*^{R} (GFY104), *vma21QQ voa1*Δ*Nat*^{R} (GCY3), and *vma21QQ-Nat*^{R} (GFY36). Colonies from the final double or triple mutant strains were analyzed for fitness defects on rich media plus 2.75 mM or 7.0 mM $ZnCl_2$ or rich media buffered to pH 7.5 plus 50 mM or 100 mM $CaCl_2$. The haploid deletion library was also tested and scored under identical media conditions. Fitness defects of single knockout strains were noted and considered when determining synthetic growth effects. *HPH1* and *ORM2* (shown in boldface type) were chosen for further study. A comprehensive gene ontology (GO) analysis for enriched categories of genes can be found in Table S2.

WT but the *vma21QQ hph1*Δ *hph2*Δ mutant was fully sensitive under these conditions and unable to grow (Figure 2C). Interestingly, the *hph1*Δ *hph2*Δ double mutant did not show any sensitivity to 4.0 mM $ZnCl_2$ but displayed a dramatic shift in sensitivity between 4.0 mM and 5.0 mM $ZnCl_2$.

The SGA screens also identified cells lacking *ORM2* as an enhancer of the assembly factor mutant strains *vma21QQ* and *vma21QQ voa1*Δ on media containing either zinc or calcium. The *orm2*Δ was recreated in SF838-1Dα cells expressing *vma21QQ* and tested on media containing 25 mM calcium buffered to pH 7.5. Loss of *ORM2* in *vma21QQ* yeast caused a slight increase in the sensitivity of this strain compared to *vma21QQ* yeast (Figure 3A). *ORM2* has a homolog in *S. cerevisiae*, *ORM1*, and the double *orm1*Δ *orm2*Δ mutant shows synthetic growth defects under various environmental stress conditions including elevated mercury or the reducing agent DTT (Hjelmqvist *et al.* 2002). We tested whether a loss of both *ORM1* and *ORM2* caused an increase in sensitivity to 25 mM calcium at pH 7.5. While deletion of *ORM1* did not result in any growth defect, yeast deleted for *ORM2* were partially sensitive under these conditions (Figure 3B). However, the *orm1*Δ *orm2*Δ double mutant displayed a synthetic growth defect under these conditions. Due to the high similarity between *ORM1* and *ORM2* (~67% identical), we tested whether *ORM1* and *ORM2* are functionally redundant. Overexpression of Orm1p was able to fully rescue the growth defect of an *orm2*Δ strain (Figure 3C). These data suggest that *ORM1* and *ORM2* are a functionally redundant gene pair; we chose to examine the effect of a loss of both Orm1p and Orm2p on the V-ATPase.

Finally, we compared the growth of *vma21QQ* and *orm1*Δ *orm2*Δ yeast to the triple *vma21QQ orm1*Δ *orm2*Δ mutant using less stringent conditions of unbuffered 100 mM $CaCl_2$. Since a loss of both *ORM1* and *ORM2* was only sensitive under stringent growth conditions, we tested whether reducing V-ATPase function using the *vma21QQ* mutant would result in a more dramatic growth phenotype. Similar to the *HPH1/2* genes, a loss of both *ORM* genes in *vma21QQ* yeast caused a severe growth defect (Figure 3D). This suggests that the *ORM* genes are required when V-ATPase activity is reduced.

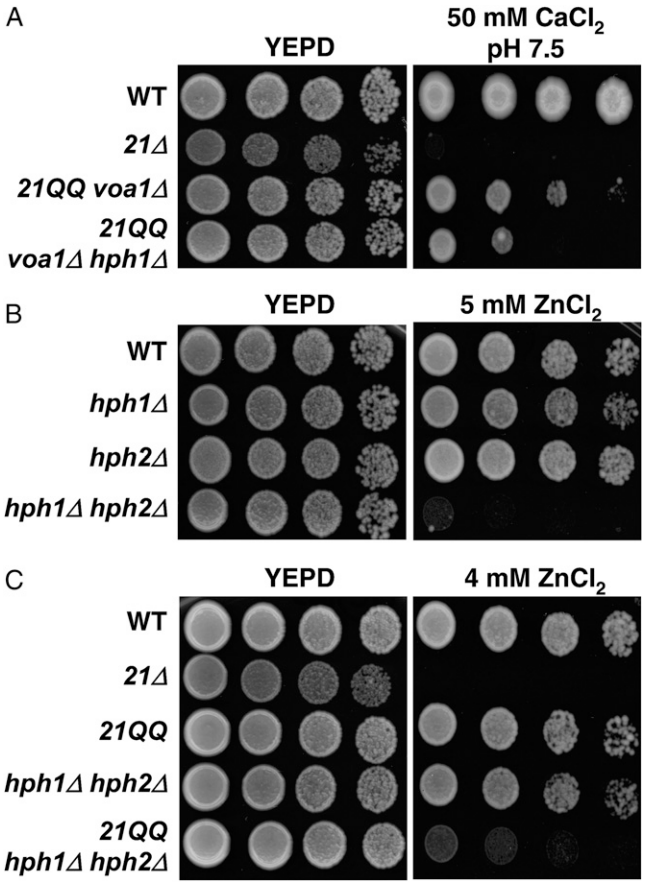

FIGURE 2.—*HPH1* and *HPH2* display synthetic growth defects with V_0 assembly mutants. (A) Exponentially growing cultures of wild type (WT; SF838-1Dα), *vma21*Δ (*21*Δ; *TASY006*), *vma21QQ voa::Hyg*^{R} (*21QQ voa1*Δ; MRY5), and *vma21QQ voa1::Hyg*^{R} *hph1*Δ (*21QQ voa1*Δ *hph1*Δ; GFY173) were serially diluted and spotted onto rich media buffered to pH 5.0 or rich media buffered to pH 7.5 plus 50 mM $CaCl_2$. (B) Exponentially growing cultures of wild type, *hph1*Δ (*hph1*Δ; GFY164), *hph2*Δ (*hph2*Δ; GFY165), and *hph1*Δ *hph2*Δ (*hph1*Δ *hph2*Δ; GFY166) were spotted onto rich media or rich media plus 5.0 mM $ZnCl_2$. (C) Cultures of wild type, *vma21*Δ, *vma21QQ* (*21QQ*; LGY183), *hph1*Δ *hph2*Δ, and *vma21QQ hph1*Δ *hph2*Δ (*21QQ hph1*Δ *hph2*Δ; GFY167) were serially diluted and spotted onto rich media buffered to pH 5.0 or rich media plus 4.0 mM $ZnCl_2$.

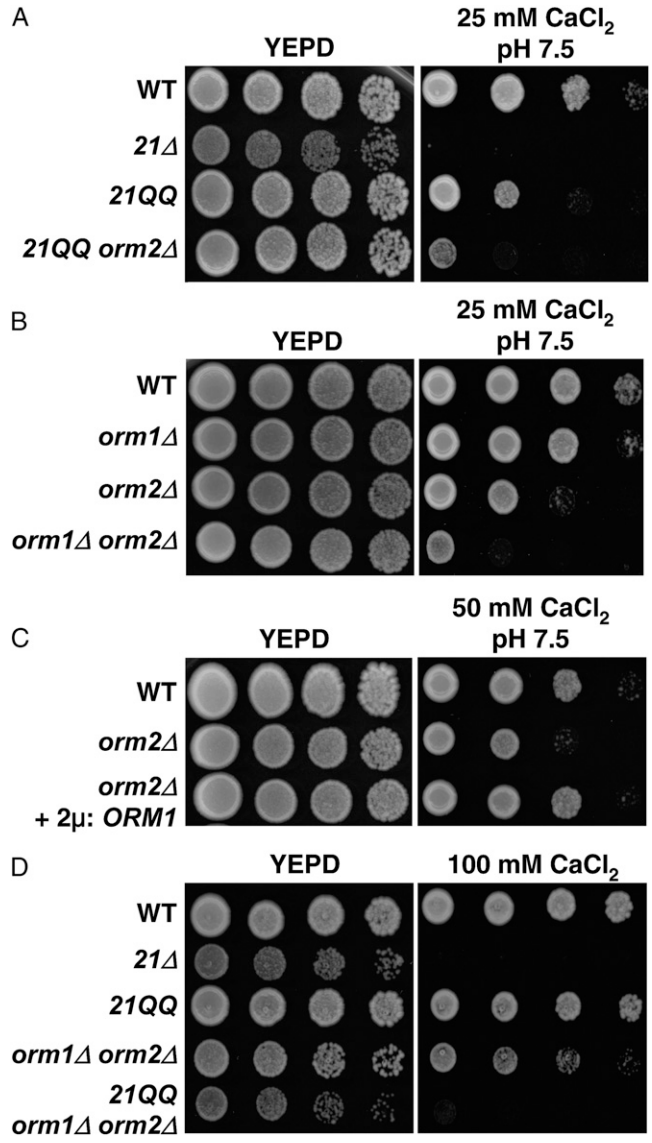

FIGURE 3.—*ORM1* and *ORM2* display synthetic growth effects in cells expressing *vma21QQ*. (A) Exponentially growing cultures of wild type (WT; SF838-1Dα), *vma21*Δ (*21*Δ; TASY006), *vma21QQ* (*21QQ*; LGY183), and *vma21QQ orm2*Δ (*21QQ orm2*Δ; GFY171) were serially diluted and spotted onto rich media buffered to pH 5.0 or rich media buffered to pH 7.5 plus 25 mM $CaCl_2$. (B) Cultures of wild type, *orm1*Δ (*orm1*Δ; GFY168), *orm2*Δ (*orm2*Δ; GFY169), and orm*1*Δ *orm2*Δ (*orm1*Δ *orm2*Δ; GFY170) spotted onto rich media and rich media buffered to pH 7.5 plus 25 mM $CaCl_2$. (C) Cultures of wild type, *orm2*Δ, and *orm2*Δ transformed with a high-copy vector expressing *ORM1* were spotted onto rich media and rich media buffered to pH 7.5 plus 50 mM $CaCl_2$. (D) Exponentially growing cultures of wild type, *vma21*Δ, *vma21QQ*, *orm1*Δ *orm2*Δ, and *vma21QQ orm1*Δ *orm2*Δ (*21QQ orm1*Δ *orm2*Δ; GFY172) were serially diluted and spotted onto rich media buffered to pH 5.0 or rich media plus 100 mM $CaCl_2$.

Vacuolar acidification, V_0 assembly, and V-ATPase localization are normal in *HPH* and *ORM* mutants: Yeast disrupted for V-ATPase function show decreases in vacuolar acidification (DAVIS-KAPLAN *et al.* 2006; RYAN *et al.* 2008). To determine whether the growth defects seen with both the *HPH* and *ORM* mutants result from a loss of V-ATPase function, we assayed vacuolar acidification by fluorescent staining with quinacrine (Figure 4). Wild-type yeast displayed accumulation of quinacrine within the acidified vacuole while *vma21*Δ yeast showed no quinacrine staining. As previously shown, yeast mutant for either *vma21QQ* or *voa1*Δ displayed wild-type levels of quinacrine staining and vacuolar acidification (RYAN *et al.* 2008; Figure 4). As expected, the *vma21QQ voa1*Δ double mutant accumulated a very low level of quinacrine (Figure 4). Surprisingly, both the double mutants (*hph1*Δ *hph2*Δ and *orm1*Δ *orm2*Δ) and the triple mutant (*vma21QQ hph1*Δ *hph2*Δ) had fully acidified vacuoles (Figure 4). Only the *vma21QQ orm1*Δ

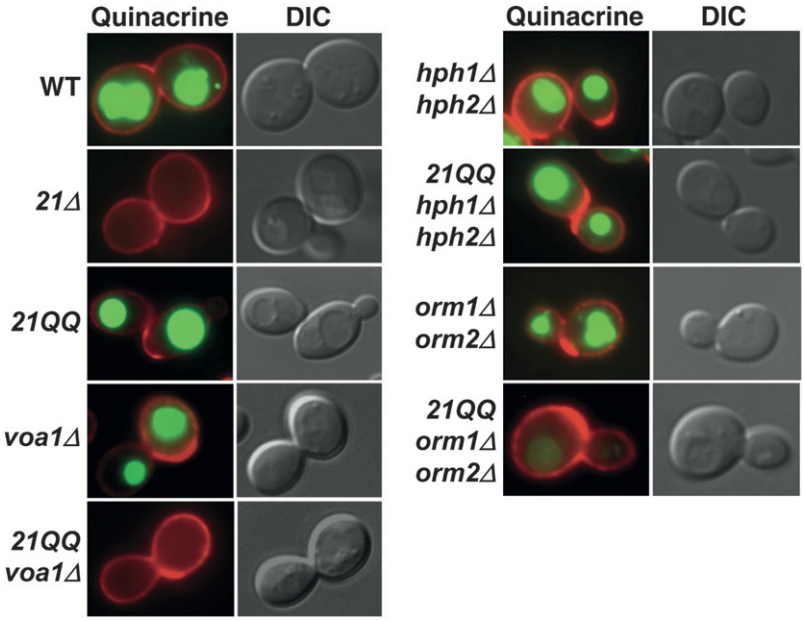

Figure 4.—Loss of *HPH1/HPH2* or *ORM1/ORM2* does not result in a loss of vacuolar acidification. Exponentially growing cultures of wild type (WT; SF838-1Dα), *vma21*Δ (*21*Δ; TASY006), *vma21QQ* (*21QQ*; LGY183), *voa1::H* (*voa1*Δ; MRY14), *vma21QQ voa1::H* (*21QQ voa1*Δ; MRY5), *hph1*Δ *hph2*Δ (*hph1*Δ *hph2*Δ; GFY166), and *vma21QQ hph1*Δ *hph2*Δ (*21QQ hph1*Δ *hph2*Δ; GFY167), *orm1*Δ *orm1*Δ (*orm1*Δ *orm2*Δ; GFY170), and *vma21QQ orm1*Δ *orm2*Δ (*21QQ orm1*Δ *orm2*Δ; GFY172) were stained with quinacrine (green) and concanavalin A-tetramethylrhodamine (red) and viewed by fluorescent and DIC microscopy.

*orm2*Δ mutant displayed a partial loss of quinacrine staining, indicating reduced V-ATPase function.

While there was no detectable difference in vacuolar acidification, it is possible that the *HPH* and *ORM* mutants have slightly reduced levels of the V-ATPase present on the vacuole that might not be apparent using fluorescent microscopy but still be consistent with the observed growth phenotypes. We assayed the levels of Vph1p within these mutant strains by Western blotting to examine any defects in V_0 assembly (Figure 5). In wild-type yeast, Vph1 protein is extremely stable (>4-hr half-life; Graham *et al.* 1998; Hill and Cooper 2000) and incorporated into the V_0 subcomplex. However, Vph1p is rapidly degraded (25–30 min half-life) if there is a V_0 assembly defect in the ER (Graham *et al.* 1998; Hill and Cooper 2000). As predicted, the levels of Vph1p in *vma21*Δ yeast were greatly reduced compared to wild-type levels. In contrast, *voa1*Δ, *hph1*Δ *hph2*Δ, and *orm1*Δ *orm2*Δ yeast all displayed wild-type levels of Vph1p. This result indicates there is no V_0 assembly defect in these strains that would result in increased turnover of Vph1p. The *vma21QQ* mutant showed a slight decrease in Vph1p levels. Careful analysis has shown that this decrease was mirrored in *HPH* and *ORM* mutant strains also containing the *vma21QQ* mutation (*vma21QQ hph1*Δ *hph2*Δ and *vma21QQ orm1*Δ *orm2*Δ). Only *vma21QQ voa1*Δ yeast showed a clear reduction in Vph1p that was greater than that seen in the *vma21QQ* mutant. The ER-resident protein Dpm1p was probed as a loading control. The steady-state levels of the V_1 subunit Vma1p did not change in any of the queried mutants.

The localization of the V-ATPase was also examined in both the *ORM* and *HPH* mutant strains. Yeast expressing both the V_0 subunit Vph1p-GFP and the V_1 subunit Vma2p-mCherry were visualized by fluorescent microscopy. In wild-type yeast, Vph1p-GFP localized to the limiting membrane of the vacuole and colocalized with Vma2p-mCherry (Figure 6). There was also a pool of Vma2p-mCherry staining within the cytosol in a diffuse pattern. In *vma21*Δ yeast, Vph1p-GFP was found in both cortical and perinuclear ER structures and Vma2p-mCherry was only localized within the cytosol. Yeast mutant for *orm1*Δ *orm2*Δ showed both V_0 and V_1 localized to the vacuolar membrane similar to wild-type cells (Figure 6). Strains mutant for *hph1*Δ *hph2*Δ localized Vph1p-GFP to the vacuole (data not shown).

Loss of the *ORM* genes (but not the *HPH* genes) results in reduced V-ATPase enzyme activity: Since it is possible that the growth defects seen in the *HPH* and *ORM* strains could result from defects in V-ATPase enzyme function (rather than from assembly defects), we performed V-ATPase activity assays on isolated vacuole membranes in these mutant strains. We measured vacuole membranes from the *hph1*Δ *hph2*Δ strain to have 88% V-ATPase activity, whereas the *orm1*Δ *orm2*Δ mutant had 67% activity relative to wild-type yeast (Table 4). We also tested V-ATPase enzyme activity for the *hph1*Δ *hph2*Δ mutant in a separate genetic background (BY4741) and found no difference from wild-type vacuole membranes (116% of WT; Table 4). We determined the *vma21QQ* mutant activity to be 22% of wild-type yeast despite the appearance of fully acidified vacuoles. The double *vma21QQ voa1*Δ mutant showed a dramatic decrease to 9%. The *vma21QQ orm1*Δ *orm2*Δ triple mutant had a comparable reduction of V-ATPase activity to 8% relative to wild-type yeast. These results indicate that the Hph proteins do not affect the activity of the V-ATPase and that the Orm proteins are required for full V-ATPase function.

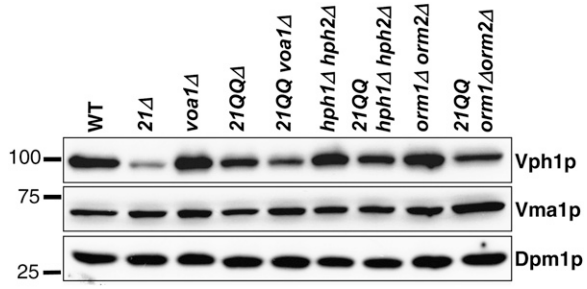

FIGURE 5.—Vph1p levels are not reduced in strains lacking either *HPH1/HPH2* or *ORM1/ORM2*. Whole cell extracts were prepared from wild type (WT; SF838-1Dα), *vma21*Δ (*21*Δ; TASY006), *vma21QQ* (*21QQ*; LGY183), *voa1::H* (*voa1*Δ; MRY14), *vma21QQ voa1::H* (*21QQ voa1*Δ; MRY5), *hph1*Δ *hph2*Δ (*hph1*Δ *hph2*Δ; GFY166), and *vma21QQ hph1*Δ *hph2*Δ (*21QQ hph1*Δ *hph2*Δ; GFY167), *orm1*Δ *orm1*Δ (*orm1*Δ *orm2*Δ; GFY170), and *vma21QQ orm1*Δ *orm2*Δ (*21QQ orm1*Δ *orm2*Δ; GFY172). Proteins were separated by SDS–PAGE and probed with anti-Vph1p and anti-Vma1p antibodies. Anti-Dpm1p antibody was used as a loading control. The molecular mass (kilodaltons) of the nearest marker is shown on the left.

The Orm proteins function in sphingolipid regulation: Two reports have recently demonstrated that Orm1p and Orm2p are negative regulators of the serine palmitoyltransferase (SPT) complex responsible for the first and rate-limiting enzymatic step of sphingolipid synthesis (BRESLOW *et al.* 2010; HAN *et al.* 2010). Since loss of Orm1p and Orm2p has been shown to result in increased sphingolipid production (BRESLOW *et al.* 2010; HAN *et al.* 2010), we tested whether inhibition of the SPT complex alleviated the defects seen in an *orm1*Δ *orm2*Δ mutant. Tsc3p is a small protein that associates with the SPT enzyme and is required for full activity of this complex (GABLE *et al.* 2000). We deleted *TSC3* in the *orm1*Δ *orm2*Δ mutant and tested the triple mutant strain on media containing elevated calcium and buffered to pH 7.5 (Figure 7A). Yeast lacking *TSC3* did not display any growth defect under these conditions. However, loss of *TSC3* allowed for increased growth of the *orm1*Δ *orm2*Δ strain. Additionally, suppression by deletion of *TSC3* was specific to the *orm1*Δ *orm2*Δ mutant, as loss of this regulator did not suppress the calcium sensitivity of the *vma21QQ voa1*Δ mutant (Figure 7B). These results suggest that the growth defects seen in the *orm1*Δ *orm2*Δ mutant strain are due to perturbation of sphingolipid synthesis.

DISCUSSION

The goal of this study was to identify additional factors that contribute to V-ATPase function that may have been missed by previous forward genetic screens. The power of enhancer and suppressor screens is evident from work in both *Drosophila melanogaster* and *Caenorhabditis elegans* where it is often necessary to use a sensitized background to uncover new genetic pathways (JORGENSEN and MANGO 2002; ST JOHNSTON 2002). In the case of the yeast V-ATPase, parallel genetic pathways are most likely not the main obstacles for identifying subtle effectors of this complex. Instead, the V-ATPase enzyme within the cell requires a dramatic decrease in enzyme function or assembly before cellular growth phenotypes become evident (RYAN *et al.* 2008). The discovery of the fourth and fifth factors that participate in V_0 assembly (Pkr1p and Voa1p) demonstrates the complexity of the assembly processes required for the V-ATPase enzyme complex. While Voa1p has been shown to physically associate with the V_0 subcomplex in the ER (RYAN *et al.* 2008), no physical association has been characterized for Pkr1p despite a strong genetic link to the assembly factor Vma21p (GRAHAM and STEVENS 1998; DAVIS-KAPLAN *et al.* 2006; data not shown). Growth phenotypes associated with perturbation of the V-ATPase are only evident upon a significant reduction in enzyme activity to ~20% of wild type as in the case of the mutant assembly factor allele, *vma21QQ* (HILL and STEVENS 1994). This retrieval-defective mutant allele of the highly conserved assembly factor,

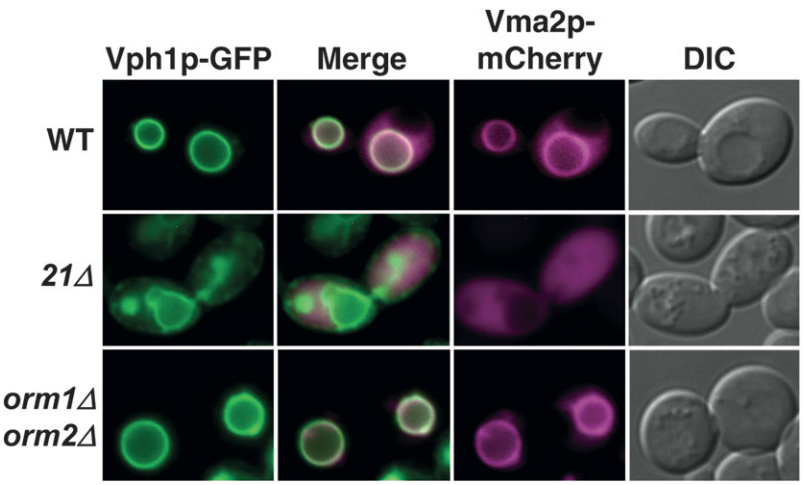

FIGURE 6.—V_1 and V_0 are localized to the vacuole membrane in *Orm* mutant yeast. A single mCherry was integrated at the *VMA2* locus in the following strains: wild type (WT; GFY304), *vma21*Δ (*21*Δ; GFY305), and *orm1*Δ *orm2*Δ (*orm1*Δ *orm2*Δ; GFY302). Yeast strains also contained a vector expressing Vph1p-GFP (pGF87). Exponentially growing cells were visualized by fluorescent and DIC microscopy.

TABLE 4

V-ATPase activity and quinacrine staining of mutants

Strain	% wild-type ATPase activity	Quinacrine
Wild type (SF838-1Dα)	100	++++
Wild type (BY4741)	100	++++[a]
*vma21*Δ	1 ± 0.3 (1)[d]	—
*hph1*Δ *hph2*Δ (SF838-1Dα)	88 ± 6 (4)[b]	++++
*hph1*Δ *hph2*Δ (BY4741)	116 ± 0.7 (1)[d]	++++[a]
*orm1*Δ *orm2*Δ	67 ± 6 (3)	++++
*voa1*Δ	75[c]	++++
vma21QQ	22 ± 1 (3)	++++
*vma21QQ voa1*Δ	9 ± 0.5 (2)	+
*vma21QQ orm1*Δ *orm2*Δ	8 ± 0.5 (2)	++

Loss of both *ORM1* and *ORM2* results in a decrease in V-ATPase activity. Activity assays were performed for wild-type strains (WT; SF838-1Dα and WT; BY4741), *vma21*Δ (*vma21*Δ; TASY006), *vma21QQ* (*vma21QQ*; LGY183), *voa1::H* (*voa1*Δ; MRY14), *orm1*Δ *orm1*Δ (*orm1*Δ *orm2*Δ; GFY170), *vma21QQ voa1::H* (*vma21QQ voa1*Δ; MRY5), *hph1*Δ *hph2*Δ SF838-1Dα (*hph1*Δ *hph2*Δ; GFY166), *hph1*Δ *hph2*Δ BY4741 (*hph1*Δ *hph2*Δ; GFY181), and *vma21QQ orm1*Δ *orm2*Δ (*vma21QQ orm1*Δ *orm2*Δ; GFY172). A continuous, coupled spectrophotometric assay (Conibear and Stevens 2002) was used to assay freshly prepared vacuole membranes for concanamycin A-sensitive ATPase activity. The wild-type strain SF838-1Dα had an average specific activity of 0.817 μmol min^{-1} mg^{-1} (average of $n = 7$ independent vacuole isolations) and the wild-type strain BY4741 has a specific activity of 0.836 μmol min^{-1} mg^{-1} (1 vacuole isolation). The specific activity of mutant samples was divided by the wild-type specific activity measurement for each independent vacuolar preparation to produce a relative percentage. For samples prepared more than once (biological replicates indicated in parentheses), the different percentages were averaged to produce the percentage of wild-type activity measurements ± the standard error of the mean. Quinacrine staining is derived from Figure 3.

[a] Data not shown.

[b] Three of four measurements for *hph1*Δ *hph2*Δ (SF838-1Dα) averaged 97% of wild type.

[c] From Ryan *et al.* (2008).

[d] For strains with only a single biological preparation, the error is expressed as the standard deviation of technical replicates.

Vma21p, is a unique scenario to serve as a genetic tool for enhancer (and suppressor) screens because (i) the levels of functional V-ATPase are sufficiently low to allow for phenotypic scoring, and (ii) the V-ATPase is not compromised for enzyme function, but rather, is defective for assembly due to the limited supply of Vma21p in the ER.

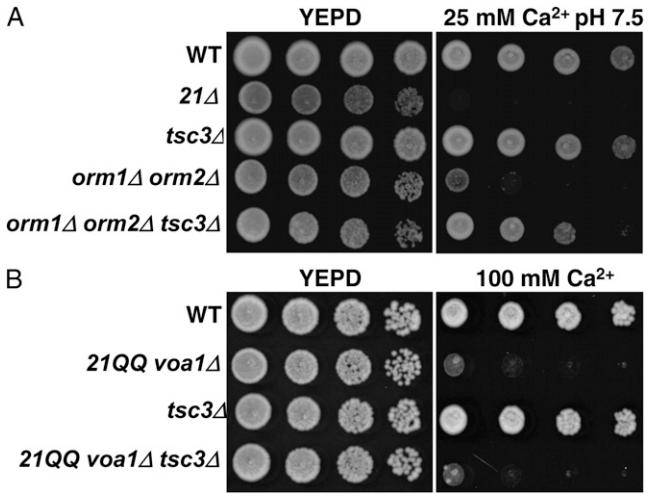

Figure 7.—Orm sensitivity to buffered calcium media can be suppressed by inhibition of sphingolipid biogenesis. (A) Cultures of wild type (WT; SF838-1Dα), *vma21*Δ (*21*Δ; TASY006), *tsc3*Δ (*tsc3*Δ; GFY174), *orm1*Δ *orm2*Δ (*orm1*Δ *orm2*Δ; GFY170), and *orm1*Δ *orm2*Δ *tsc3*Δ (*orm1*Δ *orm2*Δ *tsc3*Δ; GFY175) were spotted onto rich media and media containing 25 mM $CaCl_2$ buffered to pH 7.5. (B) Wild type, *vma21QQ voa1*Δ (*21QQ voa1*Δ; MRY5), *tsc3*Δ, and *vma21QQ voa1*Δ *tsc3*Δ (*21QQ voa1*Δ *tsc3*Δ; GFY313) yeast were spotted onto rich media and media containing 100 mM $CaCl_2$.

In performing genome-wide enhancer screens with the *vma21QQ* and *vma21QQ voa1*Δ alleles, a large number of genes involved in vesicular trafficking pathways, endosomal sorting complex required for transport (ESCRT) machinery, vesicle formation, and vacuolar morphology were identified. Deletion of some trafficking-related genes has been shown to result in sensitivity to zinc, calcium, or alkaline conditions (Serrano *et al.* 2004; Sambade *et al.* 2005; Pagani *et al.* 2007). Our strategy for screening effectively detected reduced V-ATPase activity levels to ~10% of wild-type yeast (scored as <50% of activity in the *vma21QQ* mutant strain). It is therefore not surprising that we have identified additional genes involved in trafficking pathways that were not previously found in forward genetic screens. For instance, many of the vacuolar protein sorting (VPS) genes have not been identified in previous genome-wide screens for Vma^- phenotypes (Sambade *et al.* 2005). The genetic relationship between these sorting pathways and vacuolar acidification most likely results from aberrant sorting of the V-ATPase. There are many ways by which disruption of vesicular trafficking can result in mislocalization of the V-ATPase enzyme. For example, loss of the AAA-ATPase Vps4p results in an aberrant multivesicular body that traps vacuole-bound

cargo in this compartment (Raymond *et al.* 1992). In addition, loss of the syntaxin Pep12p (another class of trafficking mutants) results in mislocalization of Vph1p (Gerrard *et al.* 2000). If the V-ATPase is not targeted to the vacuolar membrane, the pH gradient necessary to drive the sequestration of excess metals is not established, and the result is an increased sensitivity in our screen. Due to the complexity of protein sorting from the Golgi to the vacuole, there are many components that are required for proper transport of the V-ATPase to the vacuole membrane (Bowers and Stevens 2005). It will be of interest to determine whether disruption of other trafficking pathways is able to affect metal sensitivity without perturbation of V-ATPase localization and function.

We chose to characterize two gene families, *HPH1* and *ORM2*, whose protein products had been previously reported to localize to the ER; both have homologs within budding yeast, *HPH2* and *ORM1*, respectively (Hjelmqvist *et al.* 2002; Heath *et al.* 2004). *HPH1* and *HPH2* have been characterized as new components of calcineurin signaling (Heath *et al.* 2004). Genetic screens have also found that deletion of any of the essential subunits of the V-ATPase is synthetic lethal with a loss of calcineurin (Tanida *et al.* 1995; Parsons *et al.* 2004). We therefore investigated the involvement of the Hph proteins in the function and/or assembly of the V-ATPase complex in the ER.

HPH1 and *HPH2* have been previously reported to be functionally redundant and sensitive to high salinity or alkaline conditions (Heath *et al.* 2004). We have found a unique set of growth phenotypes associated with a loss of *HPH1* and *HPH2* on media containing excess metals. The *hph1*Δ *hph2*Δ mutant did not display any sensitivity to elevated calcium (data not shown) yet displayed a nonlinear shift in zinc sensitivity. This was unusual, as our previously observed V-ATPase mutants with a partial reduction in function, *pkr1*Δ, *vma21QQ*, and *vma21QQ voa1*Δ (data not shown), exhibit growth defects on *both* zinc and calcium to varying degrees and have a gradual response to increasing concentrations of $ZnCl_2$. Preliminary work has also demonstrated that the zinc sensitivity of the *hph1*Δ *hph2*Δ mutant was not completely dependent on calcineurin (data not shown). On the basis of our results, we propose that the growth defect of *hph1*Δ *hph2*Δ yeast on $ZnCl_2$ likely results from a V-ATPase independent mechanism. It is unclear whether the zinc sensitivity in *Hph* mutants results from an effect on vacuole-localized Zn^{2+} transportation or some other mechanism.

Genome-wide screens for zinc or calcium (at pH 7.5) sensitivity have found genes that do not directly contribute to V-ATPase function yet show sensitivity to excess metals (Sambade *et al.* 2005; Pagani *et al.* 2007). An example is deletion of the vacuolar zinc transporter Zrc1p, which confers zinc sensitivity even though vacuolar acidification is normal (data not shown). Also, a loss of the serine protease Kex2p results in both calcium and zinc sensitivity yet does not cause any defect in vacuolar acidification (Sambade *et al.* 2005). Identifying which genetic pathways are directly linked to metal sensitivity independent of V-ATPase function will require further study.

The Orm proteins are also functionally redundant, integral membrane proteins that localize to the ER in yeast (data not shown). Since loss of both *ORM* genes caused a reduction in vacuolar acidification and V-ATPase enzyme activity in the context of the *vma21QQ* mutation, we propose that Orm1p and Orm2p are necessary for full V-ATPase function. However, the phenotype associated with disruption of only the *ORM* genes does not completely phenocopy a loss of other assembly factors (such as *PKR1* or the combination *vma21QQ voa1*Δ). Key differences highlight the potential mechanism through which the Orm proteins may impact the V-ATPase including the lack of an apparent V_0 assembly defect. It is unlikely that the Orm proteins transiently participate in V_0 assembly of the V-ATPase, as we were unable to determine any physical association of Orm2p with the Vma21p-V_0 subcomplex (data not shown).

We also examined whether a variety of cargo proteins (including both subdomains of the V-ATPase) were aberrantly targeted upon a loss of the Orm proteins. Resident ER (Vma21p), Golgi (Vps10p), plasma membrane (Pma1p, Ste3p, and Snf3p), and vacuolar proteins (Sna3p, Zrt3p, Vcx1p, Pho8p, and Cps1p) did not display changes in localization patterns compared to wild-type yeast (data not shown). Consistent with these data, we found normal V_1V_0 localization of the V-ATPase to the vacuole membrane, suggesting an indirect involvement of Orm1p and Orm2p. A more likely scenario involves perturbation of V-ATPase function through other cellular pathways.

Recently, two studies have characterized Orm1p and Orm2p as negative regulators of sphingolipid synthesis (Breslow *et al.* 2010; Han *et al.* 2010). Both groups have reported that the Orm proteins physically associate with and regulate the SPT complex in the ER. Interestingly, inhibition of the SPT enzyme complex was found to alleviate phenotypes associated with a loss of *ORM1* and *ORM2*, including cold sensitivity and sensitivity to tunicamycin (Han *et al.* 2010). Our data are consistent with these findings and it is likely that *ORM1* and *ORM2* indirectly affect V-ATPase function through perturbation of sphingolipid production. This interpretation is in agreement with the effect of the lipid environment on the assembly, transport, or function of various enzymes including the amino acid permease Gap1p (Lauwers *et al.* 2007), uracil permease Fur4p (Hearn *et al.* 2003), and plasma membrane H^+-ATPase Pma1p (Wang and Chang 2002; Gaigg *et al.* 2006).

Also, deletion of two components of the fatty acid elongation pathway required for sphingolipid C26 acyl

group synthesis (*fen1*Δ and *sur4*Δ) resulted in perturbation of vacuolar acidification, a decrease in V-ATPase enzyme activity, and a functionally compromised V_1 domain (Chung *et al.* 2003). This previous study reported destabilization of the V-ATPase; specifically, a portion of the V_1 subdomain dissociates from the membrane during vacuole membrane preparation of the *sur4*Δ mutant. Since loss of the Orm proteins results in a similar change in the lipidome as *sur4*Δ yeast (Breslow *et al.* 2010), loss of the V_1 subdomain during vacuolar preparation could explain why *vma21QQ orm1*Δ *orm2*Δ cells display levels of V-ATPase activity similar to *vma21Q voa1*Δ yeast but higher vacuolar acidification *in vivo*. Since they are negative regulators, deletion of *ORM1* and *ORM2* results in an increase in the sphingolipid composition of the cell (Breslow *et al.* 2010). Loss of the Orm proteins results in a subtle decrease in V-ATPase function and this differs from both the *sur4*Δ and *fen1*Δ mutations. However, this connection between sphingolipid regulation and V-ATPase function would have been missed in previous forward genetic screens. Overproduction of sphingolipids likely results in an altered lipid environment for the V-ATPase as sphingolipids play crucial roles for many cellular functions (Hanada 2003; Cowart and Obeid 2007).

The use of sensitized genetic backgrounds to identify factors that have subtle effects on V-ATPase function has revealed genes involved in a variety of cellular pathways. We have identified the Orm proteins and implicated sphingolipid regulation as important contributors to full V-ATPase enzyme activity. Future genome-wide screens that specifically assay V-ATPase function will aid in separating genes, like *HPH1* and *HPH2*, which do not directly affect enzyme activity, from those that are dedicated effectors of V-ATPase assembly, transport, or enzyme function. Finally, further characterization of the precise mechanism by which alteration of sphingolipids and the cellular lipid composition affect function of the V-ATPase will be of great interest and provide a more complete understanding of this crucial molecular machine.

We thank Laurie Graham and Emily Coonrod for reading the manuscript and members of the Stevens lab for discussions. This work was supported by the National Institutes of Health grant GM-38006 (to T.H.S.) and training grant S T32 GM-007257 (to G.C.F.).

Note added in proof: A very recent study implicated *HPH1*/*HPH2* in V-ATPase biogenesis (Piña *et al.*, Euk. Cell, **10:** 63–71, 2011). Piña *et al.* report that Vph1p is degraded equally rapidly in *vma21*Δ and *hph1*Δ *hph2*Δ mutants (Piña *et al.* 2011; Figure 3D), in contrast to our findings that Vph1p levels are normal in *hph1*Δ *hph2*Δ mutants, but significantly reduced in *vma21*Δ mutants (our Figure 5). Rapid turnover of Vph1p in *hph1*Δ *hph2*Δ yeast is inconsistent with near-normal growth in the presence of 250 mM Ca^{2+} (Piña *et al.* 2011; Figure 3A) and 4 mM Zn^{2+} (our Figure 2C). Additionally, the stability of Vph1p in wild-type yeast determined by Piña *et al.* is inconsistent with previously published measurements (>5 hours; Graham *et al.*, 1998). Finally and most importantly, our study reports that vacuoles from *hph1*Δ *hph2*Δ yeast (in two different genetic backgrounds) have 100% of wild-type V-ATPase activity, whereas *vma21*Δ cells have no measureable V-ATPase activity (our Table 4). In contrast to Piña *et al.*, based on our data, we conclude that the *HPH1*/*HPH2* genes do not play a role in V-ATPase biogenesis.

LITERATURE CITED

Bowers, K., and T. H. Stevens, 2005 Protein transport from the late Golgi to the vacuole in the yeast *Saccharomyces cerevisiae*. Biochim. Biophys. Acta **1744:** 438–454.

Breslow, D. K., S. R. Collins, B. Bodenmiller, R. Aebersold, K. Simons *et al.*, 2010 Orm family proteins mediate sphingolipid homeostasis. Nature **463:** 1048–1053.

Chung, J. H., R. L. Lester and R. C. Dickson, 2003 Sphingolipid requirement for generation of a functional V_1 component of the vacuolar ATPase. J. Biol. Chem. **278:** 28872–28881.

Compton, M. A., L. A. Graham and T. H. Stevens, 2006 Vma9p (subunit e) is an integral membrane V_0 subunit of the yeast V-ATPase. J. Biol. Chem. **281:** 15312–15319.

Conibear, E., and T. H. Stevens, 2002 Studying yeast vacuoles. Methods Enzymol. **351:** 408–432.

Cowart, L. A., and L. M. Obeid, 2007 Yeast sphingolipids: recent developments in understanding biosynthesis, regulation, and function. Biochim. Biophys. Acta **1771:** 421–431.

Davis-Kaplan, S. R., M. A. Compton, A. R. Flannery, D. M. Ward, J. Kaplan *et al.*, 2006 *PRK1* encodes an assembly factor for the yeast V-type ATPase. J. Biol. Chem. **281:** 32025–32035.

Eide, D. J., S. Clarke, T. M. Nair, M. Gehl, M. Gribskov *et al.*, 2005 Characterization of the yeast ionome: a genome-wide analysis of nutrient mineral and trace element homeostasis in *Saccharomyces cerevisiae*. Genome Biol. **6:** R77.

Flannery, A. R., L. A. Graham and T. H. Stevens, 2004 Topological characterization of the c, c′, and c′′ subunits of the vacuolar ATPase from the yeast *Saccharomyces cerevisiae*. J. Biol. Chem. **279:** 39856–39862.

Forgac, M., 2007 Vacuolar ATPases: rotary proton pumps in physiology and pathophysiology. Nat. Rev. Mol. Cell Biol. **8:** 917–929.

Frattini, A., P. J. Orchard, C. Sobacchi, S. Giliani, M. Abinun *et al.*, 2000 Defects in TCIRG1 subunit of the vacuolar proton pump are responsible for a subset of human autosomal recessive osteopetrosis. Nat. Genet. **25:** 343–346.

Gable, K., H. Slife, D. Bacikova, E. Monaghan and T. M. Dunn, 2000 Tsc3p is an 80-amino acid protein associated with serine palmitoyltransferase and required for optimal enzyme activity. J. Biol. Chem. **275:** 7597–7603.

Gaigg, B., A. Toulmay and R. Schneiter, 2006 Very long-chain fatty acid-containing lipids rather than sphingolipids *per se* are required for raft association and stable surface transport of newly synthesized plasma membrane ATPase in yeast. J. Biol. Chem. **281:** 34135–34145.

Gerrard, S. R., B. P. Levi and T. H. Stevens, 2000 Pep12p is a multifunctional yeast syntaxin that controls entry of biosynthetic, endocytic and retrograde traffic into the prevacuolar compartment. Traffic **1:** 259–269.

Graham, L. A., K. J. Hill and T. H. Stevens, 1998 Assembly of the yeast vacuolar H^+-ATPase occurs in the endoplasmic reticulum and requires a Vma12p/Vma22p assembly complex. J. Cell Biol. **142:** 39–49.

Graham, L. A., A. R. Flannery and T. H. Stevens, 2003 Structure and assembly of the yeast V-ATPase. J. Bioenerg. Biomembr. **35:** 301–312.

Goldstein, A. L., and J. H. Mccuster, 1999 Three new dominant drug resistance cassettes for gene disruption in *Saccharomyces cerevisiae*. Yeast **15:** 1541–1553.

Han, S., M. A. Lone, R. Schneiter and A. Chang, 2010 Orm1 and Orm2 are conserved endoplasmic reticulum membrane proteins regulating lipid homeostasis and protein quality control. Proc. Natl. Acad. Sci. USA **107:** 5851–5856.

Hanada, K., 2003 Serine palmitoyltransferase, a key enzyme of sphingolipid metabolism. Biochim. Biophys. Acta **1632:** 16–30.

Hearn, J. D., R. L. Lester and R. C. Dickson, 2003 The uracil transporter Fur4p associates with lipid rafts. J. Biol. Chem. **278:** 3679–3686.

Heath, V. L., S. L. Shaw, S. Roy and M. S. Cyert, 2004 Hph1p and Hph2p, novel components of calcineurin-mediated stress responses in *Saccharomyces cerevisiae*. Eukaryot. Cell **3:** 695–704.

Hill, J. E., A. M. Myers, T. J. Koerner and A. Tzagoloff, 1986 Yeast/E. coli shuttle vectors with multiple unique restriction sites. Yeast **2:** 163–167.

Hill, K., and A. A. Cooper, 2000 Degradation of unassembled Vph1p reveals novel aspects of the yeast ER quality control system. EMBO J. **19:** 550–561.

Hill, K. J., and T. H. Stevens, 1994 Vma21p is a yeast membrane protein retained in the endoplasmic reticulum by a di-lysine motif and is required for the assembly of the vacuolar H^+-ATPase complex. Mol. Biol. Cell **5:** 1039–1050.

Hill, K. J., and T. H. Stevens, 1995 Vma22p is a novel endoplasmic reticulum associated protein required for assembly of the yeast vacuolar H^+-ATPase complex. J. Biol. Chem. **270:** 22329–22336.

Hirata, R., N. Umemoto, M. N. Ho, Y. Ohya, T. H. Stevens *et al.*, 1993 *VMA12* is essential for assembly of the vacuolar H(+)-ATPase subunits onto the vacuolar membrane in *Saccharomyces cerevisiae*. J. Biol. Chem. **268:** 961–967.

Hirata, T., A. Iwamoto-Kihara, G. H. Sun-Wada, T. Okajima, Y. Wada *et al.*, 2003 Subunit rotation of vacuolar-type proton pumping ATPase: relative rotation of the G as to c subunit. J. Biol. Chem. **278:** 23714–23719.

Hjelmqvist, L., M. Tuson, G. Marfany, E. Herrero, S. Balcells *et al.*, 2002 ORMDL proteins are a conserved new family of endoplasmic reticulum membrane proteins. Genome Biol. **3:** RESEARCH0027.

Ho, M. N., K. J. Hill, M. A. Lindorfer and T. H. Stevens, 1993 Isolation of vacuolar membrane H(+)-ATPase-deficient yeast mutants; the *VMA5* and *VMA4* genes are essential for assembly and activity of the vacuolar H(+)-ATPase. J. Biol. Chem. **268:** 221–227.

Imamura, H., M. Takeda, S. Funamoto, K. Shimabukuro, M. Yoshida *et al.*, 2005 Rotation scheme of V_1-motor is different from that of F_1-motor. Proc. Natl. Acad. Sci. USA **13:** 17929–17933.

Jorgensen, E. M., and S. E. Mango, 2002 The art and design of genetic screens: *Caenorhabditis elegans*. Nat. Rev. Genet. **3:** 356–369.

Kane, P. M., 2006 The where, when, and how of organelle acidification by the yeast vacuolar H^+-V-ATPase. Microbiol. Mol. Biol. Rev. **70:** 177–191.

Kane, P. M., 2007 The long physiological reach of the yeast vacuolar H^+-ATPase. J. Bioenerg. Biomembr. **39:** 415–421.

Karet, F. E., K. E. Finberg, R. D. Nelson, A. Nayir, H. Mocan *et al.*, 1999 Mutations in the gene encoding B1 subunit of H^+-ATPase cause renal tubular acidosis with sensorineural deafness. Nat. Genet. **21:** 84–90.

Klionsky, D. J., P. K. Herman, and S. D. Emr, 1990 The fungal vacuole: composition, function, and biogenesis. Microbiol. Rev. **54:** 266–292.

Lauwers, E. G. Grossman, and B. André, 2007 Evidence for coupled biogenesis of yeast Gap1 permease and sphingolipids: essential role in transport activity and normal control by ubquitination. Mol. Biol. Cell **18:** 3068–3080.

MacDiarmid, C. W., M. A. Milanick and D. J. Eide, 2002 Biochemical properties of vacuolar zinc transport systems of *Saccharomyces cerevisiae*. J. Biol. Chem. **277:** 39187–39194.

Malkus, P., L. A. Graham, T. H. Stevens and R. Schekman, 2004 Role of Vma21p in assembly and transport of the yeast vacuolar ATPase. Mol. Biol. Cell **15:** 5075–5091.

Manolson, M. F., D. Proteau, R. A. Preston, A. Stenbit, B. T. Roberts *et al.*, 1992 The *VPH1* gene encodes a 95-kDa integral membrane polypeptide required for *in vivo* assembly and activity of the yeast vacuolar H^+-ATPase. J. Biol. Chem. **267:** 14294–14303.

Manolson, M. F., B. Wu, D. Proteau, B. E. Taillon, B. T. Roberts *et al.*, 1994 *STV1* gene encodes functional homologue of the 95-kDa yeast vacuolar H^+-ATPase subunit Vph1p. J. Biol. Chem. **269:** 14064–14074.

Markwell, M. A., S. M. Haas, L. L. Bieber and N. E. Tolbert, 1978 A modification of the Lowry procedure to simplify protein determination in membrane and lipoprotein samples. Anal. Biochem. **87:** 206–210.

Marshansky, V., and M. Futai, 2008 The V-type H^+-ATPase in vacuolar trafficking: targeting, regulation and function. Curr. Opin. Cell Biol. **20:** 1–20.

Martínez-Zaguilán, R., N. Raghunand, R. M. Lynch, W. Bellamy, G. M. Martinez *et al.*, 1999 pH and drug resistance. I. Functional expression of plasmalemmal V-type H^+-ATPase in drug-resistant human breast carcinoma cell lines. Biochem. Pharmacol. **57:** 1037–1046.

Miseta, A., R. Kellermayer, D. P. Aiello, L. Fu, and D. M. Bedwell, 1999 The vacuolar Ca^{2+}/H^+ exchanger Vcx1p/Hum1p tightly controls cytosolic Ca^{2+} levels in S. cerevisiae. FEBS Lett. **451:** 132–136.

Ohya, Y., N. Umemoto, I. Tanida, A. Ohta, H. Iida *et al.*, 1991 Calcium-sensitive *cls* mutants of *Saccharomyces cerevisiae* showing a Pet-phenotype are ascribable to defects of vacuolar membrane H(+)-ATPase activity. J. Biol. Chem. **266:** 13971–13977.

Pagani, M. A., A. Casamayor, R. Serrano, S. Atrian and J. Ariño, 2007 Disruption of iron homeostasis in *Saccharomyces cerevisiae* by high zinc levels: a genome-wide study. Mol. Microbiol. **65:** 521–537.

Parsons, A. B., R. L. Brost, H. Ding, Z. Li, C. Zhang *et al.*, 2004 Integration of chemical-genetic and genetic interaction data links bioactive compounds to celluar target pathways. Nat. Biotechnol. **22:** 62–69.

Raymond, C. K., I. Howald-Stevenson, C. A. Vater and T. H. Stevens, 1992 Morphological classification of the yeast vacuolar protein sorting mutants: evidence for a prevacuolar compartment in class E vps mutants. Mol. Biol. Cell **3:** 1389–1402.

Rothman, J. H., and T. H. Stevens, 1986 Protein sorting in yeast: mutants defective in vacuole biogenesis mislocalize vacuolar proteins into the late secretory pathway. Cell **47:** 1041–1051.

Ryan, M., L. A. Graham and T. H. Stevens, 2008 Voa1p functions in V-ATPase assembly in the yeast endoplasmic reticulum. Mol. Biol. Cell **19:** 5131–5142.

Sambade, M., M. Alba, A. M. Smardon, R. W. West and P. M. Kane, 2005 A genomic screen for yeast vacuolar membrane ATPase mutants. Genetics **170:** 1539–1551.

Sambrook, J., and D. W. Russel, 2001 *Molecular Cloning: A Laboratory Manual*, Ed 3. Cold Spring Harbor Laboratory Press, Cold Spring Harbor, NY.

Serrano, R., D. Bernal, E. Simón and J. Ariño, 2004 Copper and Iron are the limiting factors for growth of the yeast *Saccharomyces cerevisiae* in an alkaline environment. J. Biol. Chem. **279:** 19698–19704.

Shaner, N. C., R. E. Campbell, P. A. Steinbach, B. N. G. Giepmans, A. E. Palmer *et al.*, 2004 Improved monomeric red, orange and yellow fluorescent proteins derived from *Discosoma* sp. red fluorescent protein. Nat. Biotechnol. **22:** 1567–1572.

Sikorski, R. S., and P. Hieter, 1989 A system of shuttle vectors and yeast host strains designed for efficient manipulation of DNA in *Saccharomyces cerevisiae*. Genetics **122:** 19–27.

Simons, R. W., F. Houman and N. Kleckner, 1987 Improved single and multicopy lac-based cloning vectors for protein and operon fusions. Gene **53:** 85–96.

St Johnston, D., 2002 The art and design of genetic screens: *Drosophila melanogaster*. Nat. Rev. Genet. **3:** 176–188.

Tanida, I., A. Hasegawa, H. Iida, Y. Ohya and Y. Anraku, 1995 Cooperation of calcineurin and vacuolar H(+)-ATPase in intracellular Ca^{2+} homeostasis of yeast cells. J. Biol. Chem. **270:** 10113–10119.

Tomashek, J. J., L. A. Graham, M. U. Hutchins, T. H. Stevens and D. J. Klionsky, 1997 V_1-situated stalk subunits of the yeast vacuolar proton-translocating ATPase. J. Biol. Chem. **272:** 26787–26793.

Tong, A. H., and C. Boone, 2006 Synthetic genetic array analysis in *Saccharomyces cerevisiae*. Methods Mol. Biol. **313:** 171–192.

Tong, A. H., M. Evangelista, A. B. Parsons, H. Xu, G. D. Bader *et al.*, 2001 Systematic genetic analysis with ordered arrays of yeast deletions mutants. Science **294:** 2364–2368.

Uchida, E., Y. Oshumi and Y. Anraku, 1985 Purification and properties of H^+-translocating, Mg^{+2}-adenosine triphosphatase from vacuolar membrane of *Saccharomyces cerevisiae*. J. Biol. Chem. **260:** 1090–1095.

Wang, Q., and A. Chang, 2002 Sphingoid base synthesis is required for oligomerization and cell surface stability of the yeast plasma membrane ATPase, Pma1. Proc. Natl. Acad. Sci. USA **99:** 12853–12858.

Weisman, L. S., R. Bacallao and W. Wickner, 1987 Multiple methods of visualizing the yeast vacuole permit evaluation of its morphology and inheritance during the cell cycle. J. Cell Biol. **105:** 1539–1547.

Yokoyama, K., M. Nakano, H. Imamura, M. Yoshida and M. Tamakoshi, 2003 Rotation of the proteolipid ring in the V-ATPase. J. Biol. Chem. **278:** 24255–24258.

Communicating editor: M. D. Rose

GENETICS

Supporting Information
http://www.genetics.org/cgi/content/full/genetics.110.125567/DC1.

A Genome-Wide Enhancer Screen Implicates Sphingolipid Composition in Vacuolar ATPase Function in *Saccharomyces cerevisiae*

Gregory C. Finnigan, Margret Ryan and Tom H. Stevens

DOI: 10.1534/genetics.110.125567

TABLE S1

Genes identified by genome-wide SGA screens for V-ATPase effectors

Gene	ORF	*vma21QQ::Nat^R*	*vma21QQ voa1::Hyg^R*	*vma21QQ voa1Δ::Nat^R*
AAT2	YLR027C	X		X
ACO1	YLR304C	X		
ACO2	YJL200C	X		
ADA2	YDR448W	X		
ADI1	YMR009W		X	
ADO1	YJR105W			X
AGE2	YIL044C		X	
AIM14	YGL160W			X
ALG6	YOR002W	X		X
ALG8	YOR067C	X		X
ANP1	YEL036C	X		
APE3	YBR286W			X
API2	YDR525W		X	
APL5	YPL195W	X	X	
APL6	YGR261C		X	X
APM1	YPL259C		X	
APM3	YBR288C	X	X	
APS3	YJL024C	X	X	
ARF1	YDL192W		X	
ARG2	YJL071W		X	
ARG82	YDR173C	X		
ARL1	YBR164C	X	X	X
ARL3	YPL051W		X	X
ARO1	YDR127W	X	X	
ARO2	YGL148W	X	X	X
ARO7	YPR060C	X	X	X
ARP6	YLR085C		X	X
ARR4	YDL100C		X	
ASC1	YMR116C		X	X
ASF1	YJL115W		X	
ATG15	YCR068W			X
ATG21	YPL100W			X
ATG27	YJL178C		X	
ATG8	YBL078C		X	
ATS1	YAL020C		X	X
AVT7	YIL088C		X	
BAP2	YBR068C		X	
BCK1	YJL095W			X

BCK2	YER167W	X	X	X
BDF1	YLR399C			X
BEM1	YBR200W	X		
BEM2	YER155C	X	X	X
BEM4	YPL161C	X	X	X
BMH1	YER177W		X	
BRE1	YDL074C	X	X	X
BRE2	YLR015W		X	
BSD2	YBR290W		X	X
BST1	YFL025C		X	
BTS1	YPL069C	X		
BUD14	YAR014C		X	
BUD30	YDL151C	X		
CAJ1	YER048C		X	
CAT5	YOR125C			X
CBF1	YJR060W	X	X	X
CCC2	YDR270W		X	
CCR4	YAL021C	X		X
CCW12	YLR110C		X	
CCZ1	YBR131W	X	X	
CDC50	YCR094W	X		
CEX1	YOR112W		X	
CHD1	YER164W			X
CHS5	YLR330W		X	X
CHS6	YJL099W			X
CKA1	YIL035C		X	
CKB1	YGL019W	X	X	X
CKB2	YOR039W	X	X	X
CLA4	YNL298W		X	X
CNB1	YKL190W			X
CNE1	YAL058W		X	
COG5	YNL051W		X	X
COG6	YNL041C		X	
COG7	YGL005C		X	X
COG8	YML071C		X	X
COY1	YKL179C		X	
CPR2	YHR057C			X
CPR7	YJR032W		X	
CRZ1	YNL027W	X	X	X
CSF1	YLR087C	X	X	X
CSG2	YBR036C	X	X	X

CTF18	YMR078C		X	
CTF4	YPR135W			X
CTK1	YKL139W	X	X	X
CUE1	YMR264W		X	
CWH41	YGL027C		X	
CYK3	YDL117W		X	
CYS3	YAL012W	X		
DAL81	YIR023W			X
DBF2	YGR092W		X	
DBP7	YKR024C	X		X
DFG16	YOR030W			X
DFG5	YMR238W	X		
DIA2	YOR080W		X	
DLT1	YMR126C	X	X	X
DOA1	YKL213C		X	
DOM34	YNL001W		X	
DPH1	YIL103W		X	
DPH2	YKL191W		X	
DPH5	YLR172C		X	
DRS2	YAL026C	X	X	X
DST1	YGL043W		X	
DUF1	YOL087C			X
EAF3	YPR023C			X
EAF7	YNL136W			X
ECM38	YLR299W		X	
ECM40	YMR062C			X
EFT2	YDR385W		X	
ELF1	YKL160W			X
ELM1	YKL048C		X	X
ELP2	YGR200C		X	
ELP3	YPL086C		X	
ELP4	YPL101W		X	
ELP6	YMR312W		X	X
EMC1	YCL045C		X	
ERD1	YDR414C			X
ERG3	YLR056W	X	X	X
ERG6	YML008C	X	X	X
ERP3	YDL018C	X		
ERV46	YAL042W		X	
FET3	YMR058W	X	X	
FET4	YMR319C			X

FIG4	YNL325C		X	
FKS1	YLR342W		X	
FLC2	YAL053W	X		
FMC1	YIL098C			X
FMP21	YBR269C			X
FPS1	YLL043W			X
FRA1	YLL029W			X
FRT1	YOR324C			X
FTR1	YER145C		X	
FUI1	YBL042C		X	
FUM1	YPL262W	X		
FYV10	YIL097W			X
GAL11	YOL051W			X
GAS1	YMR307W		X	
GCN1	YGL195W		X	
GCR2	YNL199C		X	
GCS1	YDL226C		X	
GEF1	YJR040W		X	
GET1	YGL020C	X	X	
GET2	YER083C	X	X	X
GIM4	YEL003W	X		
GIS4	YML006C		X	
GLY1	YEL046C	X		
GOS1	YHL031C	X	X	
GPA2	YER020W		X	
GSF2	YML048W			X
GSG1	YDR108W	X	X	X
GSH1	YJL101C	X	X	
GSH2	YOL049W		X	
GUP1	YGL084C		X	X
GVP36	YIL041W		X	
GYP1	YOR070C	X	X	X
HAC1	YFL031W	X		
HAL5	YJL165C		X	X
HCR1	YLR192C	X	X	
HEX3	YDL013W		X	
HGH1	YGR187C		X	
HMT1	YBR034C		X	
HOC1	YJR075W	X		
HSC82	YMR186W		X	
HTZ1	YOL012C		X	X

ICE2	YIL090W	X	X	
IDH2	YOR136W	X	X	
IKI3	YLR384C		X	
ILM1	YJR118C		X	
ILV1	YER086W			X
IMG2	YCR071C	X		
INO2	YDR123C		X	
INP53	YOR109W		X	
IOC2	YLR095C		X	
IRA2	YOL081W	X		
IRC13	YOR235W		X	
IRC14	YOR135C	X	X	
IRC21	YMR073C			X
IRC25	YLR021W		X	
ISW1	YBR245C		X	
JJJ3	YJR097W		X	
KAR3	YPR141C		X	
KCS1	YDR017C	X		
KEM1	YGL173C	X	X	X
KES1	YPL145C		X	
KEX1	YGL203C			X
KEX2	YNL238W	X	X	
KRE1	YNL322C			X
KRE28	YDR532C	X	X	
KTI12	YKL110C		X	
LCL1	YPL056C	X		
LEO1	YOR123C		X	X
LGE1	YPL055C	X	X	X
LIP2	YLR239C	X	X	
LIP5	YOR196C	X		
LPD1	YFL018C			X
LSB3	YFR024C-A		X	
LSM1	YJL124C	X	X	
LSM6	YDR378C	X		
LST4	YKL176C		X	
LYS14	YDR034C	X	X	X
MAC1	YMR021C	X	X	
MAF1	YDR005C		X	
MBF1	YOR298C-A		X	
MCK1	YNL307C			X
MDM10	YAL010C		X	

MDM20	YOL076W				X
MDM34	YGL219C				X
MDY2	YOL111C	X			
MET18	YIL128W		X		
MET22	YOL064C		X		
MGA2	YIR033W		X		
MGM101	YJR144W				X
MKS1	YNL076W		X		X
MMS1	YPR164W		X		
MMS22	YLR320W		X		
MNN10	YDR245W	X	X		
MNN2	YBR015C		X		
MOG1	YJR074W		X		
MON1	YGL124C	X	X		X
MPD2	YOL088C	X			
MRC1	YCL061C		X		
MRPL35	YDR322W				X
MSC1	YML128C		X		
MSN5	YDR335W	X	X		X
MTC2	YKL098W	X	X		X
MTC4	YBR255W		X		X
MTC6	YHR151C		X		
NAM7	YMR080C				X
NBP2	YDR162C	X	X		X
NCS2	YNL119W		X		
NCS6	YGL211W		X		
NHX1	YDR456W	X			
NMD2	YHR077C		X		
NPL3	YDR432W				X
NPT1	YOR209C				X
NST1	YNL091W		X		
NUP133	YKR082W		X		
OCA5	YHL029C		X		
OCT1	YKL134C				X
OPI1	YHL020C		X		X
OPI8	YKR035C	X	X		X
ORM2	YLR350W	X	X		X
OST3	YOR085W	X	X		
OST4	YDL232W		X		X
PAR32	YDL173W				X
PBS2	YJL128C				X

PCL6	YER059W			X
PCT1	YGR202C			X
PDA1	YER178W		X	
PDB1	YBR221C	X		
PER1	YCR044C		X	X
PET191	YJR034W			X
PEX31	YGR004W	X		X
PFK1	YGR240C			X
PGD1	YGL025C			X
PHO2	YDL106C		X	
PHO4	YFR034C	X	X	X
PHO80	YOL001W	X	X	X
PHO81	YGR233C	X	X	
PHO85	YPL031C	X		X
PHO86	YJL117W	X	X	X
PIL1	YGR086C			X
PIN4	YBL051C		X	
PKR1	YMR123W		X	
PMC1	YGL006W	X	X	X
PMP3	YDR276C		X	
POC4	YPL144W		X	
POP2	YNR052C	X		X
PPM1	YDR435C			X
PPR1	YLR014C		X	
PSD2	YGR170W		X	
PSP2	YML017W		X	
PTK2	YJR059W			X
QRI8	YMR022W		X	
RAV1	YJR033C		X	X
RAV2	YDR202C	X	X	X
RBG2	YGR173W			X
RCY1	YJL204C		X	
RIF1	YBR275C		X	
RIM101	YHL027W		X	X
RIM20	YOR275C		X	X
RIM21	YNL294C		X	
RIM8	YGL045W		X	X
RIM9	YMR063W		X	X
RKR1	YMR247C		X	
RMD8	YFR048W		X	
RNR4	YGR180C			X

ROT2	YBR229C		X	
RPA34	YJL148W		X	
RPL13A	YDL082W		X	
RPL13B	YMR142C			X
RPL17B	YJL177W			X
RPL22B	YFL035C-B			X
RPL29	YFR032C-A		X	
RPL2A	YFR031C-A		X	
RPL41B	YDL133C-A		X	
RPL9A	YGL147C		X	
RPN4	YDL020C		X	
RPO41	YFL036W		X	
RPP1A	YDL081C	X		
RPS11A	YDR025W			X
RPS11B	YBR048W		X	
RPS16B	YDL083C		X	
RPS19A	YOL121C			X
RPS21B	YJL136C	X	X	X
RPS24A	YER074W			X
RPS27B	YHR021C		X	
RPS28B	YLR264W		X	
RPS29B	YDL061C		X	
RPS4A	YJR145C	X		
RPS4B	YHR203C		X	
RPS6B	YBR181C		X	
RRF1	YHR038W			X
RRT2	YBR246W		X	
RSM28	YDR494W			X
RTG1	YOL067C		X	X
RTG2	YGL252C	X	X	X
RTG3	YBL103C		X	X
RTS1	YOR014W	X	X	X
RTT103	YDR289C		X	X
RTT109	YLL002W		X	
RUD3	YOR216C		X	
RVS161	YCR009C		X	
SAC1	YKL212W		X	X
SAC3	YDR159W		X	X
SAC7	YDR389W	X	X	X
SAP155	YFR040W		X	X
SAT4	YCR008W		X	

SBP1	YHL034C			X	
SCJ1	YMR214W			X	
SCS2	YER120W			X	
SCW10	YMR305C				X
SDC1	YDR469W	X			
SEC22	YLR268W	X		X	
SEC28	YIL076W			X	
SEC66	YBR171W	X		X	X
SER2	YGR208W	X		X	
SET2	YJL168C			X	X
SHE1	YBL031W			X	
SHE4	YOR035C			X	X
SHP1	YBL058W				X
SIM1	YIL123W			X	
SIN4	YNL236W			X	
SIS2	YKR072C	X		X	X
SIT1	YEL065W			X	
SKG1	YKR100C			X	
SKN7	YHR206W			X	X
SLA1	YBL007C				X
SMF1	YOL122C				X
SMF3	YLR034C				X
SMI1	YGR229C	X		X	
SMP2	YMR165C	X		X	
SNA2	YDR525W-A			X	
SNF1	YDR477W			X	
SNF11	YDR073W				X
SNF2	YOR290C	X			X
SNF4	YGL115W				X
SNF5	YBR289W	X			
SNF6	YHL025W			X	
SNX4	YJL036W				X
SOD2	YHR008C				X
SOH1	YGL127C			X	
SOK2	YMR016C	X			
SOY1	YBR194W	X			
SPE1	YKL184W			X	
SPE3	YPR069C			X	
SPF1	YEL031W			X	X
SPT3	YDR392W			X	
SPT4	YGR063C				X

SQS1	YNL224C			X	
SRB2	YHR041C			X	X
SRB8	YCR081W			X	
SRN2	YLR119W				X
SRO7	YPR032W			X	
SSE1	YPL106C			X	
STO1	YMR125W				X
STP1	YDR463W	X			X
STV1	YMR054W	X			
SUR1	YPL057C			X	X
SUR4	YLR372W				X
SWC3	YAL011W			X	
SWC5	YBR231C			X	X
SWD1	YAR003W	X			
SWD3	YBR175W	X			
SWF1	YDR126W			X	X
SWI4	YER111C	X		X	X
SWI6	YLR182W				X
SWP82	YFL049W				X
SWR1	YDR334W			X	
SYS1	YJL004C	X		X	X
TAE1	YBR261C			X	
TCO89	YPL180W				X
TDA4	YJR116W				X
TEF4	YKL081W			X	X
THR1	YHR025W	X		X	X
THR4	YCR053W	X		X	X
TLG2	YOL018C	X			
TMA17	YDL110C			X	
TMA23	YMR269W			X	
TOP1	YOL006C			X	
TOS2	YGR221C			X	
TOS9	YEL007W				X
TPD3	YAL016W	X			
TPM1	YNL079C			X	
TPS1	YBR126C			X	X
TRK1	YJL129C				X
TRP1	YDR007W			X	
TRP2	YER090W			X	
TRP4	YDR354W			X	
TSR2	YLR435W			X	

TUF1	YOR187W	X		
UBA3	YPR066W	X		
UBA4	YHR111W		X	
UBP13	YBL067C	X	X	
UBP14	YBR058C		X	
UBP15	YMR304W	X	X	
UBP3	YER151C			X
UBP6	YFR010W		X	
UBX4	YMR067C		X	
UFD2	YDL190C		X	
UME6	YDR207C	X	X	X
UPF3	YGR072W		X	
URA4	YLR420W			X
URE2	YNL229C		X	
URM1	YIL008W		X	
VAC14	YLR386W		X	X
VAC8	YEL013W	X	X	X
VAM10	YOR068C	X	X	X
VAM6	YDL077C	X	X	
VAM7	YGL212W		X	
VHS2	YIL135C			X
VID21	YDR359C		X	
VID22	YLR373C		X	
VPH1	YOR270C	X	X	X
VPS1	YKR001C	X		
VPS13	YLL040C		X	
VPS17	YOR132W	X	X	
VPS19	YDR323C	X		
VPS2	YKL002W	X		
VPS21	YOR089C		X	X
VPS22	YPL002C	X		
VPS23	YCL008C	X		
VPS24	YKL041W	X	X	X
VPS25	YJR102C	X		
VPS26	YJL053W	X	X	X
VPS27	YNR006W	X	X	
VPS29	YHR012W	X	X	X
VPS3	YDR495C	X		
VPS33	YLR396C	X		X
VPS35	YJL154C	X	X	X
VPS36	YLR417W	X		

VPS4	YPR173C	X	X	X
VPS41	YDR080W		X	
VPS46	YKR035W-A	X	X	X
VPS5	YOR069W	X	X	X
VPS52	YDR484W	X		
VPS53	YJL029C	X		
VPS55	YJR044C		X	X
VPS6	YOR036W	X		
VPS60	YDR486C		X	X
VPS62	YGR141W		X	
VPS71	YML041C			X
VPS72	YDR485C			X
VPS73	YGL104C		X	
VPS9	YML097C		X	
VTA1	YLR181C		X	X
VTC1	YER072W	X	X	X
VTC4	YJL012C	X	X	X
VTS1	YOR359W		X	X
XRS2	YDR369C		X	
YAK1	YJL141C			X
YAL058C-A	YAL058C-A		X	
YAP1801	YHR161C		X	
YAR029W	YAR029W		X	
YBL071C	YBL071C			X
YBL094C	YBL094C	X		
YBR174C	YBR174C	X		
YBR226C	YBR226C		X	
YBR284W	YBR284W			X
YCK3	YER123W	X	X	X
YCL046W	YCL046W		X	
YCR007C	YCR007C		X	
YCR061W	YCR061W			X
YDJ1	YNL064C		X	
YDL172C	YDL172C			X
YDL218W	YDL218W	X		
YDR048C	YDR048C		X	
YDR049W	YDR049W		X	
YDR089W	YDR089W	X		
YDR203W	YDR203W	X		X
YDR269C	YDR269C		X	
YDR271C	YDR271C	X	X	

YDR336W	YDR336W	X			
YDR433W	YDR433W				X
YDR455C	YDR455C	X		X	
YDR537C	YDR537C				X
YEH1	YLL012W				X
YEL045C	YEL045C	X			
YER119C-A	YER119C-A			X	
YER156C	YER156C	X			
YFR024C	YFR024C			X	
YGL024W	YGL024W			X	X
YGL218W	YGL218W			X	X
YGR064W	YGR064W				X
YGR122W	YGR122W			X	
YGR237C	YGR237C			X	
YJL169W	YJL169W			X	X
YJL175W	YJL175W			X	X
YJR087W	YJR087W				X
YKE2	YLR200W	X			
YKG9	YKL069W			X	
YKL023W	YKL023W				X
YKL061W	YKL061W				X
YKL118W	YKL118W				X
YKR051W	YKR051W				X
YLR111W	YLR111W			X	
YLR143W	YLR143W			X	
YLR402W	YLR402W			X	
YML013C-A	YML013C-A			X	
YML020W	YML020W	X			
YND1	YER005W				X
YNL120C	YNL120C			X	X
YNL140C	YNL140C				X
YNL171C	YNL171C			X	
YNL198C	YNL198C			X	
YNL228W	YNL228W			X	
YNL296W	YNL296W			X	
YNR005C	YNR005C				X
YOL050C	YOL050C				X
YOR300W	YOR300W				X
YPL102C	YPL102C			X	
YPL168W	YPL168W				X
YPL205C	YPL205C	X			

YPR090W	YPR090W		X	
YPR123C	YPR123C	X	X	
YPR153W	YPR153W	X	X	X
YPT7	YML001W	X	X	X
YTA7	YGR270W		X	X
YUR1	YJL139C		X	
ZRC1	YMR243C		X	X
ZUO1	YGR285C			X

The standard gene name and systematic names of all the genes identified from the 3 SGA enhancer screens are listed. X's indicate which of the three different SGA screens genes were identified from. The three different query strains used are labeled above each column. These data include scoring of double mutants on media containing either Ca^{2+} or Zn^{2+}.

TABLE S2

Gene Ontology (GO) analysis of genes identified from enhancer SGA screens

GO ID#	GO Term	Cluster frequency	Background frequency	P-value
7034	vacuolar transport	47 out of 492 genes, 9.6%	124 out of 5797 background genes, 2.1%	4.94E-17
9987	cellular process	443 out of 492 genes, 90.0%	4336 out of 5797 background genes, 74.8%	2.56E-16
16192	vesicle-mediated transport	82 out of 492 genes, 16.7%	357 out of 5797 background genes, 6.2%	3.48E-15
65007	biological regulation	174 out of 492 genes, 35.4%	1199 out of 5797 background genes, 20.7%	1.56E-12
46907	intracellular transport	101 out of 492 genes, 20.5%	596 out of 5797 background genes, 10.3%	9.46E-10
65008	regulation of biological quality	75 out of 492 genes, 15.2%	389 out of 5797 background genes, 6.7%	2.28E-09
51649	establishment of localization in cell	105 out of 492 genes, 21.3%	648 out of 5797 background genes, 11.2%	5.71E-09
48193	Golgi vesicle transport	45 out of 492 genes, 9.1%	181 out of 5797 background genes, 3.1%	1.49E-08
51641	cellular localization	114 out of 492 genes, 23.2%	747 out of 5797 background genes, 12.9%	3.20E-08
6623	protein targeting to vacuole	26 out of 492 genes, 5.3%	71 out of 5797 background genes, 1.2%	3.57E-08
6355	regulation of transcription, DNA-dependent	74 out of 492 genes, 15.0%	406 out of 5797 background genes, 7.0%	5.71E-08
6892	post-Golgi vesicle-mediated transport	25 out of 492 genes, 5.1%	70 out of 5797 background genes, 1.2%	1.61E-07
45449	regulation of transcription	76 out of 492 genes, 15.4%	433 out of 5797 background genes, 7.5%	1.99E-07
51252	regulation of RNA metabolic process	74 out of 492 genes, 15.0%	419 out of 5797 background genes, 7.2%	2.67E-07
31326	regulation of cellular biosynthetic process	89 out of 492 genes, 18.1%	549 out of 5797 background genes, 9.5%	3.46E-07
9889	regulation of biosynthetic process	89 out of 492 genes, 18.1%	551 out of 5797 background genes, 9.5%	4.21E-07
10468	regulation of gene expression	85 out of 492 genes, 17.3%	518 out of 5797 background genes, 8.9%	5.04E-07
44249	cellular biosynthetic process	201 out of 492 genes, 40.9%	1666 out of 5797 background genes, 28.7%	9.93E-07
16197	endosome transport	23 out of 492 genes, 4.7%	65 out of 5797 background genes, 1.1%	1.10E-06

			1162 out of 5797	
51179	localization	152 out of 492 genes, 30.9%	background genes, 20.0%	1.35E-06
	regulation of macromolecule		530 out of 5797	
10556	biosynthetic process	85 out of 492 genes, 17.3%	background genes, 9.1%	1.64E-06
	regulation of cellular			
	macromolecule biosynthetic		530 out of 5797	
2000112	process	85 out of 492 genes, 17.3%	background genes, 9.1%	1.64E-06
			1690 out of 5797	
9058	biosynthetic process	202 out of 492 genes, 41.1%	background genes, 29.2%	2.09E-06
			1180 out of 5797	
19538	protein metabolic process	153 out of 492 genes, 31.1%	background genes, 20.4%	2.26E-06
			1057 out of 5797	
51234	establishment of localization	140 out of 492 genes, 28.5%	background genes, 18.2%	3.62E-06
			1030 out of 5797	
6810	transport	137 out of 492 genes, 27.8%	background genes, 17.8%	4.35E-06
	cellular macromolecule		340 out of 5797	
70727	localization	61 out of 492 genes, 12.4%	background genes, 5.9%	6.64E-06
	regulation of nucleobase,			
	nucleoside, nucleotide and nucleic		502 out of 5797	
19219	acid metabolic process	80 out of 492 genes, 16.3%	background genes, 8.7%	7.43E-06
	regulation of nitrogen compound		504 out of 5797	
51171	metabolic process	80 out of 492 genes, 16.3%	background genes, 8.7%	8.97E-06
			384 out of 5797	
8104	protein localization	66 out of 492 genes, 13.4%	background genes, 6.6%	9.07E-06
	protein retention in Golgi		11 out of 5797	
45053	apparatus	9 out of 492 genes, 1.8%	background genes, 0.2%	1.05E-05
	regulation of macromolecule		588 out of 5797	
60255	metabolic process	89 out of 492 genes, 18.1%	background genes, 10.1%	1.24E-05
			571 out of 5797	
6351	transcription, DNA-dependent	87 out of 492 genes, 17.7%	background genes, 9.8%	1.36E-05
			573 out of 5797	
32774	RNA biosynthetic process	87 out of 492 genes, 17.7%	background genes, 9.9%	1.62E-05
			324 out of 5797	
34613	cellular protein localization	58 out of 492 genes, 11.8%	background genes, 5.6%	1.78E-05
	regulation of cellular metabolic		648 out of 5797	
31323	process	95 out of 492 genes, 19.3%	background genes, 11.2%	1.91E-05
			677 out of 5797	
19222	regulation of metabolic process	98 out of 492 genes, 19.9%	background genes, 11.7%	2.10E-05
	regulation of primary metabolic		622 out of 5797	
80090	process	92 out of 492 genes, 18.7%	background genes, 10.7%	2.17E-05
6350	transcription	90 out of 492 genes, 18.3%	607 out of 5797	2.85E-05

			background genes, 10.5%	
	protein localization in Golgi		12 out of 5797	
34067	apparatus	9 out of 492 genes, 1.8%	background genes, 0.2%	3.91E-05
			26 out of 5797	
6896	Golgi to vacuole transport	13 out of 492 genes, 2.6%	background genes, 0.4%	3.94E-05
			1136 out of 5797	
44267	cellular protein metabolic process	144 out of 492 genes, 29.3%	background genes, 19.6%	4.17E-05
			499 out of 5797	
33036	macromolecule localization	77 out of 492 genes, 15.7%	background genes, 8.6%	6.36E-05
			123 out of 5797	
55082	cellular chemical homeostasis	30 out of 492 genes, 6.1%	background genes, 2.1%	6.94E-05
			123 out of 5797	
6873	cellular ion homeostasis	30 out of 492 genes, 6.1%	background genes, 2.1%	6.94E-05
			62 out of 5797	
7033	vacuole organization	20 out of 492 genes, 4.1%	background genes, 1.1%	8.36E-05
	cellular macromolecule		1231 out of 5797	
34645	biosynthetic process	152 out of 492 genes, 30.9%	background genes, 21.2%	8.90E-05
	macromolecule biosynthetic		1233 out of 5797	
9059	process	152 out of 492 genes, 30.9%	background genes, 21.3%	9.95E-05
			127 out of 5797	
50801	ion homeostasis	30 out of 492 genes, 6.1%	background genes, 2.2%	0.00015
			128 out of 5797	
48878	chemical homeostasis	30 out of 492 genes, 6.1%	background genes, 2.2%	0.00018
	regulation of transcription from		269 out of 5797	
6357	RNA polymerase II promoter	48 out of 492 genes, 9.8%	background genes, 4.6%	0.00038
	negative regulation of metabolic		253 out of 5797	
9892	process	46 out of 492 genes, 9.3%	background genes, 4.4%	0.00038
			6 out of 5797 background	
32447	protein urmylation	6 out of 492 genes, 1.2%	genes, 0.1%	0.00038
	negative regulation of cellular		230 out of 5797	
31327	biosynthetic process	43 out of 492 genes, 8.7%	background genes, 4.0%	0.00042
	negative regulation of biosynthetic		230 out of 5797	
9890	process	43 out of 492 genes, 8.7%	background genes, 4.0%	0.00042
	negative regulation of cellular		249 out of 5797	
31324	metabolic process	45 out of 492 genes, 9.1%	background genes, 4.3%	0.00062
			985 out of 5797	
50789	regulation of biological process	124 out of 492 genes, 25.2%	background genes, 17.0%	0.00083
	negative regulation of		236 out of 5797	
10605	macromolecule metabolic process	43 out of 492 genes, 8.7%	background genes, 4.1%	0.00089
			214 out of 5797	
6325	chromatin organization	40 out of 492 genes, 8.1%	background genes, 3.7%	0.00111

30003	cellular cation homeostasis	26 out of 492 genes, 5.3%	111 out of 5797 background genes, 1.9%	0.00124
16568	chromatin modification	35 out of 492 genes, 7.1%	177 out of 5797 background genes, 3.1%	0.00139
50794	regulation of cellular process	118 out of 492 genes, 24.0%	935 out of 5797 background genes, 16.1%	0.0015
6366	transcription from RNA polymerase II promoter	61 out of 492 genes, 12.4%	395 out of 5797 background genes, 6.8%	0.00177
10558	negative regulation of macromolecule biosynthetic process	40 out of 492 genes, 8.1%	218 out of 5797 background genes, 3.8%	0.00181
2000113	negative regulation of cellular macromolecule biosynthetic process	40 out of 492 genes, 8.1%	218 out of 5797 background genes, 3.8%	0.00181
19725	cellular homeostasis	30 out of 492 genes, 6.1%	142 out of 5797 background genes, 2.4%	0.00194
10629	negative regulation of gene expression	37 out of 492 genes, 7.5%	197 out of 5797 background genes, 3.4%	0.00253
55080	cation homeostasis	26 out of 492 genes, 5.3%	115 out of 5797 background genes, 2.0%	0.00253
40007	growth	30 out of 492 genes, 6.1%	144 out of 5797 background genes, 2.5%	0.00264
48519	negative regulation of biological process	56 out of 492 genes, 11.4%	356 out of 5797 background genes, 6.1%	0.00275
43486	histone exchange	7 out of 492 genes, 1.4%	10 out of 5797 background genes, 0.2%	0.00308
45934	negative regulation of nucleobase, nucleoside, nucleotide and nucleic acid metabolic process	39 out of 492 genes, 7.9%	215 out of 5797 background genes, 3.7%	0.00329
51172	negative regulation of nitrogen compound metabolic process	39 out of 492 genes, 7.9%	215 out of 5797 background genes, 3.7%	0.00329
48523	negative regulation of cellular process	55 out of 492 genes, 11.2%	350 out of 5797 background genes, 6.0%	0.00352
2097	tRNA wobble base modification	11 out of 492 genes, 2.2%	26 out of 5797 background genes, 0.4%	0.00368
2098	tRNA wobble uridine modification	11 out of 492 genes, 2.2%	26 out of 5797 background genes, 0.4%	0.00368
16043	cellular component organization	187 out of 492 genes, 38.0%	1680 out of 5797 background genes, 29.0%	0.00373
32507	maintenance of protein location in cell	13 out of 492 genes, 2.6%	36 out of 5797 background genes, 0.6%	0.00396

			194 out of 5797	
16481	negative regulation of transcription	36 out of 492 genes, 7.3%	background genes, 3.3%	0.00466
			210 out of 5797	
42592	homeostatic process	38 out of 492 genes, 7.7%	background genes, 3.6%	0.00471
	negative regulation of		187 out of 5797	
45892	transcription, DNA-dependent	35 out of 492 genes, 7.1%	background genes, 3.2%	0.00519
			18 out of 5797	
11	vacuole inheritance	9 out of 492 genes, 1.8%	background genes, 0.3%	0.00543
			85 out of 5797	
6914	autophagy	21 out of 492 genes, 4.3%	background genes, 1.5%	0.00545
	negative regulation of RNA		188 out of 5797	
51253	metabolic process	35 out of 492 genes, 7.1%	background genes, 3.2%	0.00589
			549 out of 5797	
6464	protein modification process	76 out of 492 genes, 15.4%	background genes, 9.5%	0.0065
			271 out of 5797	
6886	intracellular protein transport	45 out of 492 genes, 9.1%	background genes, 4.7%	0.00678
			38 out of 5797	
45185	maintenance of protein location	13 out of 492 genes, 2.6%	background genes, 0.7%	0.00791

Gene Ontology (GO) analysis was performed using the Saccharomyces Genome Database (SGD) "Gene Ontology Term Finder" (v. 0.83). Of the 538 genes identified from our three SGA screens, 492 were included within the GO analysis (overlapping ORFs were excluded). The GO term ID# and GO categories are listed. The cluster and background frequency are shown for each GO term and hits with p-values of less than 0.01 were included. Results are listed beginning with GO categories with the lowest p-values.